PALEOPROTEROZOIC PRESSURE-TEMPERATURE-DEFORMATION PATH IN THE NEWTON FIORD REGION, EASTERN BAFFIN ISLAND, NUNAVUT

Zoe M. Braden

Submitted in partial fulfillment of the requirements

For the degree of Bachelor of Science, Honours

Department of Earth Sciences

Dalhousie University, Halifax, Nova Scotia

March 2013

Distribution License

DalSpace requires agreement to this non-exclusive distribution license before your item can appear on DalSpace.

NON-EXCLUSIVE DISTRIBUTION LICENSE

You (the author(s) or copyright owner) grant to Dalhousie University the non-exclusive right to reproduce and distribute your submission worldwide in any medium.

You agree that Dalhousie University may, without changing the content, reformat the submission for the purpose of preservation.

You also agree that Dalhousie University may keep more than one copy of this submission for purposes of security, back-up and preservation.

You agree that the submission is your original work, and that you have the right to grant the rights contained in this license. You also agree that your submission does not, to the best of your knowledge, infringe upon anyone's copyright.

If the submission contains material for which you do not hold copyright, you agree that you have obtained the unrestricted permission of the copyright owner to grant Dalhousie University the rights required by this license, and that such third-party owned material is clearly identified and acknowledged within the text or content of the submission.

If the submission is based upon work that has been sponsored or supported by an agency or organization other than Dalhousie University, you assert that you have fulfilled any right of review or other obligations required by such contract or agreement.

Dalhousie University will clearly identify your name(s) as the author(s) or owner(s) of the submission, and will not make any alteration to the content of the files that you have submitted.

If you have questions regarding this license please contact the repository manager at dalspace@dal.ca.

Grant the distribution license by signing and dating below.

_____   _____

Name of signatory   Date

DALHOUSIE UNIVERSITY
Inspiring Minds

Department of Earth Sciences

Halifax, Nova Scotia

Canada B3H 4R2

(902) 494-2358

FAX (902) 494-6889

DATE: April 30th 2013

AUTHOR: Zoe M. Braden

TITLE: Paleoproterozoic pressure-temperature-deformation path in the Newton Fiord region, eastern Baffin Island, Nunavut

Degree: B.Sc. (Hons) Earth sciences   Convocation: May   Year: 2013

Permission is herewith granted to Dalhousie University to circulate and to have copied for non-commercial purposes, at its discretion, the above title upon the request of individuals or institutions.

_____

Signature of Author

THE AUTHOR RESERVES OTHER PUBLICATION RIGHTS, AND NEITHER THE THESIS NOR EXTENSIVE EXTRACTS FROM IT MAY BE PRINTED OR OTHERWISE REPRODUCED WITHOUT THE AUTHOR'S WRITTEN PERMISSION.

THE AUTHOR ATTESTS THAT PERMISSION HAS BEEN OBTAINED FOR THE USE OF ANY COPYRIGHTED MATERIAL APPEARING IN THIS THESIS (OTHER THAN BRIEF EXCERPTS REQUIRING ONLY PROPER ACKNOWLEDGEMENT IN SCHOLARLY WRITING) AND THAT ALL SUCH USE IS CLEARLY ACKNOWLEDGED.

Abstract

The Canada-Nunavut Geoscience office completed the first of two field seasons of a regional bedrock and surficial mapping project on Hall Peninsula, eastern Baffin Island, during the summer of 2012. Hall Peninsula is situated within the core of the Himalayan-scale Paleoproterozoic Trans-Hudson Orogen and consists of an eastern Archean orthogneiss domain and a western Paleoproterozoic metasedimentary and plutonic domain. The Newton Fiord study area is on the southwestern coast of Hall Peninsula and comprises two regions of contrasting styles of deformation within close proximity (ca. 4 km^2). The eastern study area lies on the limb of a regional F_2 fold and has experienced near-complete transposition of pre-existing fabric elements. The western study area lies in the hinge zone of a regional F_2 fold and provides a window into early deformation structures. Both areas consist generally of metasedimentary rocks, primarily pelite, intruded by orthopyroxene-monzogranite and late garnet-leucogranite.

Linked field observations and microtectonic analysis have revealed two main tectonometamorphic events each of which can be further characterized based on relative chronology of mineral growth and fabric formation. The first event, D_1/M_1, is characterized by aligned fibrolitic sillimanite inclusions (M_{1A}) in garnet porphyroblasts, followed by voluminous garnet-cordierite-bearing leucosome formation (M_{1B}). Field evidence for D_1 fabric elements is subtle but convincing where S_1 is recorded in the orthopyroxene-monzogranite but is cut by the garnet-leucogranite. Within the pelitic rocks, the M_{1A} assemblage is only preserved in garnet porphyrblasts and consists of garnet + sillimanite + K-feldspar + ilmenite + cordierite + quartz +/- rutile, whereas the M_{1B} melt assemblage is plagioclase + cordierite + K-feldspar + quartz +/- sillimanite +/- garnet. Both assemblages suggest equilibration above the biotite dehydration melting reaction. The second event, D_2/M_2, consists of moderately to shallowly west-dipping gneissosity (S_{2A}) defined by interlayered leucosome and sillimanite-biotite mesosome in the pelites. Progressive D_2 deformation resulted in moderately west-inclined F_{2B} folds associated with a strong hinge-parallel lineation defined by biotite and coarse matrix sillimanite (L_{2B}). The M_2 mineral assemblage associated with both phases of D_2 deformation consists of garnet + sillimanite + biotite + ilmenite + K-feldspar + plagioclase + quartz +/- melt, indicating equilibration below the biotite dehydration melting reaction and the addition of H_2O most likely from the breakdown of cordierite and crystallization of melt. These data suggest a relative chronology of events beginning with a weak S_1 foliation at granulite facies, which has been attributed to contact metamorphism as a result of orthopyroxene monzogranite emplacement. This led to a voluminous garnet-bearing partial melting phase. Progressive D_2 deformation evolved from the development of a strong flattening fabric into regional-scale, east-vergent folding and eventual shearing of F_2 fold limbs. D_2 deformation is likely a result of early crustal stacking transitioning into more complex basement-involved folding.

Table of Contents

List of Tables

List of Figures

Acknowledgements

"I have learned that people will forget what you said, people will forget what you did, but people will never forget how you made them feel." –Maya Angelou

The Department of Earth Sciences has felt like home for the past four years and I will never forget the time I spent here.

Mike Young's generous support and guidance, plus his unfailing sense of humour, were essential to the writing of this thesis. I would also like to thank the Canada-Nunavut Geoscience Office for providing me with the opportunity to map on Baffin Island and their continued support of this project.

Diane Skipton and Marc St-Onge provided valuable advice both in the field and over the course of analysis and writeup. Holly Steenkamp coached me through all my THERMOCALC difficulties. Thank you to Martin Gibling for providing helpful feedback, particularly with respect to the written component. Thanks also to Gabe, Julie, Nicole and Rich for their help with sample collection.

This would have been impossible without the unconditional support of my family. To the 2013 honours class, as well as Leigh, Shannon and Erin, for making this year a fun ride, thank you!

Abbreviations

Mineral	Abbreviation
Anorthite	An
Biotite	Bt
Clinopyroxene	Cpx
Cordierite	Crd
Garnet	Grt
Graphite	Gr
Grossular	Grs
Ilmenite	Ilm
K-feldspar	Kfs
Orthopyroxene	Opx
Plagioclase	Pl
Rutile	Rt
Sillimanite	Sil
Spinel	Spl
Quartz	Qtz

Mineral abbreviations after Kretz, 1983.

Geological Term	Abbreviation
Surface (foliation)	S
Line (lineation)	L
Fold	F
Metamorphic event	M
Deformation phase	D
Pressure	P
Temperature	T

Definition of Terms

Foliation: for the purpose of this thesis, foliation will refer to any planar fabric-forming structure created by tectonic processes (Fossen, 2010). This does not included primary features such as bedding.

S-tectonites: strongly deformed rock dominated by a planar fabric (Fossen, 2010).

L-tectonites: strongly deformed rock dominated by a linear fabric (Fossen, 2010).

Migmatite: literally "mixed rocks" with a schistose component and a leucocratic granitic component (Yardley, 1989). They form from the metamorphism of pelitic rocks at pressure-temperature conditions beyond the Sillimanite zone, with respect to Barrovian metamorphism. Generally the leucocratic component, alternatively known as the melt or mobilisate, forms in thin pods or veins parallel to foliation and consists of the most mobile elements present in the rock.

Fold types: the inter-limb angle is the angle between the limbs of a fold and is used to define the tightness of a fold (Ramsay & Huber, 1983). The tightness of a fold is a useful indication of strain gradient. Isoclinal to tight folds suggest high strain folding environments and open to gentle folds suggest low strain environments.

Type of Fold	Inter-limb Angle (degrees)
Gentle	180-120
Open	120-70
Close	70-30
Tight	30-0
Isoclinal	0

Table I: fold classification based on inter-limb angles. After Ramsay & Huber, 1983.

Chapter 1

INTRODUCTION

The crosscutting relationships of minerals observed at the microscopic scale reflect macroscopic metamorphic events and phases of deformation. The objective of a microstructural study is to decipher the sequence of these deformation phases in an area and define the corresponding metamorphic events in order to establish a relative pressure-temperature path (Passchier & Trouw, 2005). Planar or linear features imparted on a rock by a deviatoric stress field are used to identify deformation phases. Metamorphic events are considered to be the formation of a mineral assemblage that corresponds to particular pressure-temperature conditions (Passchier & Trouw, 2005).

Hall Peninsula, located on southeastern Baffin Island, Nunavut, represents an underexplored region of Canada's north with geoscience knowledge largely dating from the 1960s and the 1970s. The Canada-Nunavut Geoscience Office undertook the first of two field seasons of regional bedrock and surficial mapping during the summer of 2012 (Machado et al., 2013; Tremblay et al., 2013). This project aims to improve geoscience data for the region in order to encourage resource-based development.

This study aims to define the mineral growth–deformation fabric relationships in a 4 km^2 area on southwestern Hall Peninsula in order to develop a relative chronology of events. The study area straddles Newton Fiord in the western lithological domain where two sites with contrasting deformation styles were examined in detail. The objective of this study is to determine a relative chronology of metamorphic mineral growth and

deformation fabrics in order to provide context for a regional structural and metamorphic PhD project. This chronology will serve as a basis to inform any geochronological studies done on these rocks.

These structural, metamorphic and geochronology studies are intended to help place Hall Peninsula within the context of northeast Laurentia and to establish the cratonic affinity of Hall Peninsula. This will contribute to ongoing efforts to unravel the tectonometamorphic evolution of Hall Peninsula specifically and the Trans-Hudson Orogen (THO) as a whole.

The remainder of Chapter 1 covers the regional geology of the THO and Hall Peninsula and Chapter 2 presents the local geology of the study area as well as field observations. The bulk of the data acquired for this study are presented in Chapter 3, which consists of detailed petrographic description and mineral-fabric relationships. Chapter 4 presents preliminary electron microprobe data and pressure-temperature estimates. Chapter 5 outlines an evolutionary model for Newton Fiord in terms of a relative pressure-temperature path.

REGIONAL GEOLOGY

During the Early Proterozoic the THO assembled a number of disparate Archean crustal blocks. In northeastern Canada four crustal blocks comprise the assembled components of the Trans-Hudson Orogen (Fig. 1.1). The Superior Province to the south, the Rae craton to the north, the North Atlantic craton to the east and the Meta Incognita microcontinent, which occupies the intervening area (Fig. 1.1; Hoffman, 1988; St-Onge et al., 2000; 2001; 2009; Corrigan et al., 2009). Numerous evolutionary models

have been proposed for the assembly of these crustal blocks (St Onge et al., 2009; Corrigan et al., 2009; Wardle et al., 2002; Van Gool et al., 2002,) and the affinity of the Archean rocks of Hall Peninsula remains enigmatic.
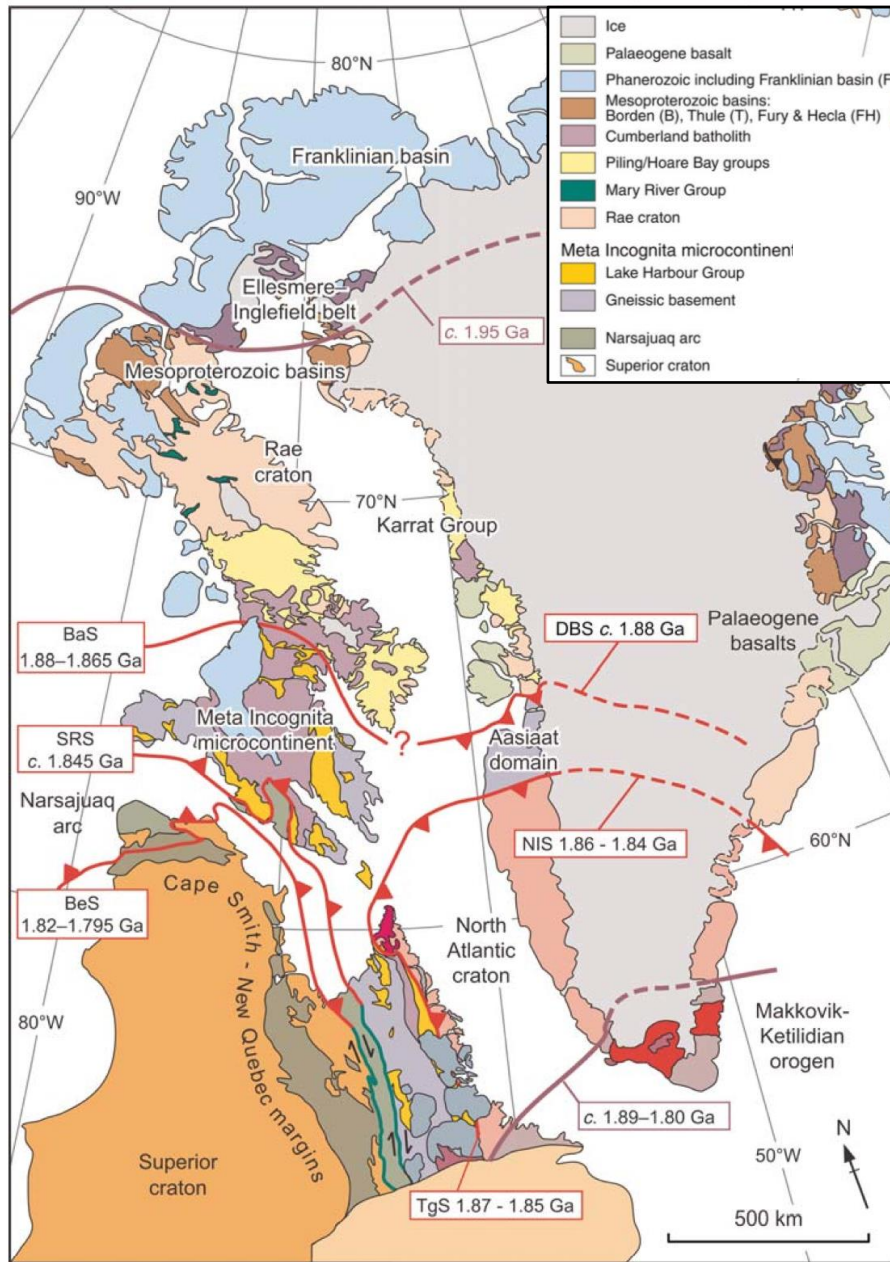
Figure 1.1: Geological map of northeast Laurentia. The northern and southern boundaries of the Trans-Hudson Orogen are marked with a purple, solid and dashed line. BaS: Baffin suture; SRS: Soper River suture; BeS: Bergeron suture; DBS: Disko Bugt suture; NIS: Nordre Isotoq steep belt; TgS: Tasiyuk gneiss suture. Modified from St-Onge et al. (2009).

Overall, the cratonic assembly youngs southward and initiated at ca. 1.93 Ga in the north and east with terminal collision of the Superior Province with the northern composite blocks at ca. 1.78 Ga (St-Onge et al., 2000; 2001; 2009; Corrigan et al., 2009; Hoffman, 1988). A large granitic pluton, known as the Cumberland Batholith, determined to be a post-accretionary batholith produced from mixed mantle and crustal sources, was emplaced between ca. 1869-1845 Ma (Whalen et al., 2010). The various phases of the Cumberland Batholith are characteristically orthopyroxene-bearing indicating emplacement temperatures greater than 750^0 C (Kilpatrick & Ellis, 1992; Whalen et al., 2010).

This study and other CNGO-sponsored thematic studies are intended to place the structural and metamorphic history of Hall Peninsula in context with the better studied surrounding regions such as South Baffin and Cumberland Peninsula (Fig. 1.1). South Baffin is the region along southernmost Baffin Island and is part of the Meta Incognita microcontinent. Two episodes of penetrative deformation affect South Baffin and include an early penetrative fabric dated at ca. 1845 Ma which evolved into tight, isoclinal folding between 1820-1805 Ma. Of note, these structures are dominantly north-dipping, south-verging.

Cumberland Peninsula is located to the north of Hall Peninsula and belongs to the Rae craton. Structures on Cumberland Peninsula are also dominantly north-dipping, south-verging. Based on in situ monazite geochronology, there is evidence of early granulite facies contact metamorphism due to pluton emplacement concurrent with early

deformation at ca. 1890 Ma (Berman et al., in press; Hamilton et al., 2012). Regionally penetrative deformation initiated at ca. 1860 and extended to ca. 1840 Ma, which has been interpreted to represent the collision between the Meta Incognita microcontinent and the Rae craton (Berman et al., in press).

South Baffin and Cumberland Peninsula share a relative chronology of events during the Paleoproterozoic, involving early granulites facies contact metamorphism and a later amphibolite facies overprint related to regionally penetrative deformation. However, South Baffin lacks the early syn-pluton emplacement deformation that is preserved on Cumberland Peninsula; both record later progressive phases of foliation development and subsequent folding. All of the ages found for South Baffin are moderately (10-15 million years) younger than those found for Cumberland. Hence, Meta Incognita was likely isolated from the Rae craton until approximately 1860-1850 Ma after which both cratons share a common tectonometamorphic history.

The tectonic evolution of Hall Peninsula has long been regarded as one of the principal puzzles key to unraveling the history of the THO. Hall Peninsula occurs at the convergence of three Archean cratons: Rae, Meta Incognita, and North Atlantic. In various tectonic models, it has been hypothesized that Hall belongs to any of these cratons. Based on work done in northern Labrador, Wardle et al. (2002) considered Hall Peninsula to be part of the North Atlantic craton via an extension of the Torngat Orogen (Fig. 1.1). Based on work done in northern Saskatchewan and Baffin Island, Corrigan et al. (2009) also considered Hall Peninsula to be part of the North Atlantic craton. Based on work done on northern Baffin Island and southwest Baffin Island, St-Onge et al.

(2009) considered Hall Peninsula to be part of Meta Incognita, with a major suture running between Cumberland Peninsula and Hall Peninsula (Fig. 1.1).

Geochronological studies in the 1990s (Scott, 1996; 1999) and more recent regional mapping (Machado et al., 2012) on Hall Peninsula have revealed two major domains based on age and dominant lithologies (Fig. 1.2). The eastern domain consists of Archean tonalite gneiss with subordinate rafts of mafic and metasedimentary rocks. In contrast, the western domain consists of Paleoproterozoic metasedimentary rocks intruded by orthopyroxene-bearing monzogranite. This orthopyroxene-monzogranite, or charnockite, is distinctly confined to the western domain and has not been observed to intrude the Archean tonalite gneiss.

The structural grain on Hall Peninsula is dominantly west-dipping in stark contrast to South Baffin to the south and Cumberland Peninsula to the north. The main west-dipping foliation affects all rocks; evidence for an earlier fabric in the eastern domain may be an inherited Archean phase of deformation. This dominant fabric is a moderately to strongly developed gneissosity that is largely controlled by lithology. East-verging folds vary in amplitude and wavelength. The intensity of this deformation varies from tight to isoclinal folds with a strongly developed axial planar fabric, to areas that appear to be largely unaffected by this later stage of folding and foliation development.
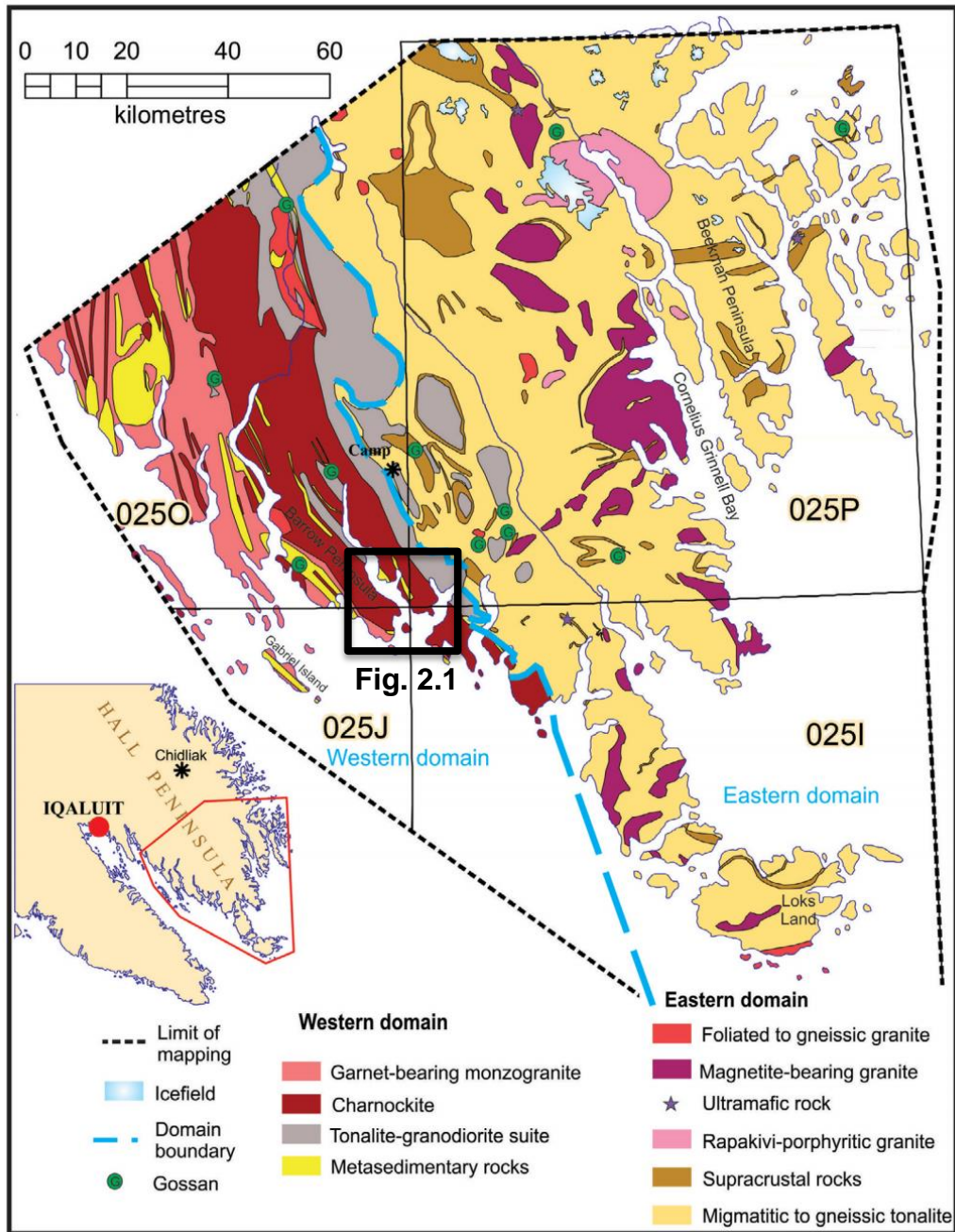
Figure 1.2: Geological map of southern Hall Peninsula, Machado et al., 2013. The blue, dashed line divides Hall Peninsula into two lithological domains. Box indicates the location of the Newton Fiord study area.

Chapter 2: Field observations & sampling

NEWTON FIORD

Newton Fiord is located along the southwestern coast of Hall Peninsula, in the western lithological domain (refer to Fig. 1.2). Figure 2.1 is an annotated aeromagnetics map (after Dumont & Dostaler, 2010) where areas of high magnetic susceptibility (red tones) generally correspond to magnetite- and orthopyroxene-bearing monzogranite, and areas of low magnetic susceptibility (blue tones) generally correspond to metasedimentary rocks. The thick, dashed white line marks the axial trace of a large wavelength regional fold that is defined by Paleoproterozoic metasedimentary rocks. The metasedimentary units are bounded by charnockite, a monzogranite with magmatic orthopyroxene, and both are cut by garnet-bearing leucogranite. The eastern study area, termed "Sillimanite Ridge", occurs on the limb of a regional fold and represents an area of nearly complete re-orientation of bedding and early deformation fabric elements by late deformation. The western study area, Barrow Peninsula, occurs in the hinge zone of a regional fold and was shielded from much of the strain attributed to regional folding, thereby providing a window into earlier deformation. Newton Fiord is in an area of voluminous partial melt, which is not traditionally targeted for metamorphic studies, however the crosscutting relations of this melt phase provide an important pin on the chronology of deformation and metamorphism.
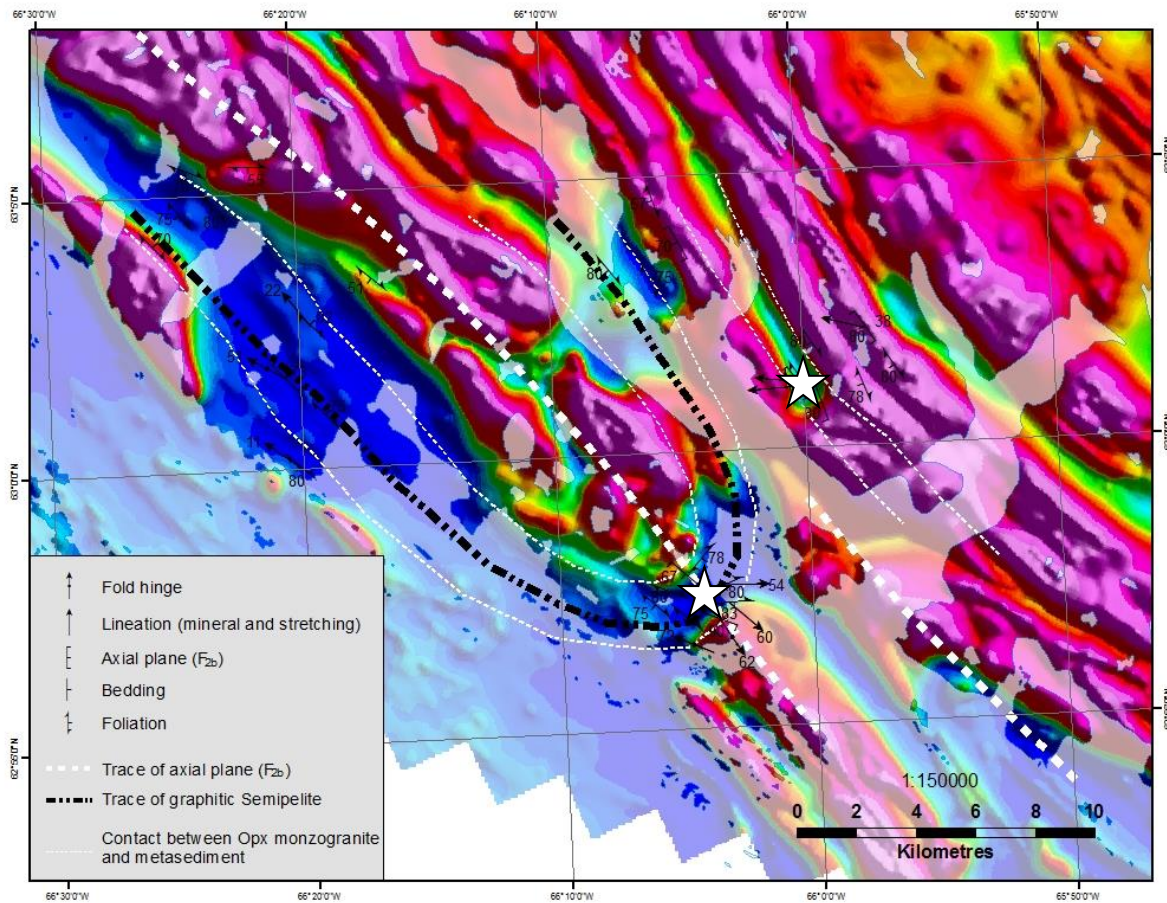
Figure 2.1: Annotated aeromagnetics map of Newton Fiord, after Dumont & Dostaler, 2010a-l. Red indicates a magnetic high, generally corresponds to orthopyroxene and magnetite-bearing monzogranite. Blue indicates a magnetic low, generally corresponds to metasedimentary rocks. Eastern star indicates Sillimanite Ridge study area location and western star indicates Barrow Peninsula study area location.

The metasedimentary units in Newton Fiord are migmatitic, rocks that formed from anatexis, or partial melting in the crust. Sawyer (2008) defined a migmatite as a rock found in medium- and high-grade metamorphic areas that can be heterogeneous at the microscopic to macroscopic scale, and that consists of two, or more, petrographically different parts. One of these parts is the leucosome, which forms from partial melting

9

and is generally quartzofeldspathic in composition. The other part is the mesosome, which is rich in ferromagnesian minerals and has mostly resisted melting. The migmatites in Newton Fiord represent an intermediate phase between purely igneous granitic textures and remnant metasedimentary textures. Despite the extensive partial melting, numerous primary sedimentary textures can be recognized such as bedding, differences in lithologic compositions such as pelite, semi-pelite and psammite, and even cross-bedding and graded bedding in rare circumstances.

Throughout the western domain of Hall Peninsula there is a strong link between the garnet-leucogranite melt phase and pelite and psammite units. A progressive transition (Fig. 2.2) from mesosome-dominated pelite to leucosome-dominated migmatite to purely igneous garnet-leucogranite can be seen over the span of several tens of metres though a sharp boundary is rarely observed.
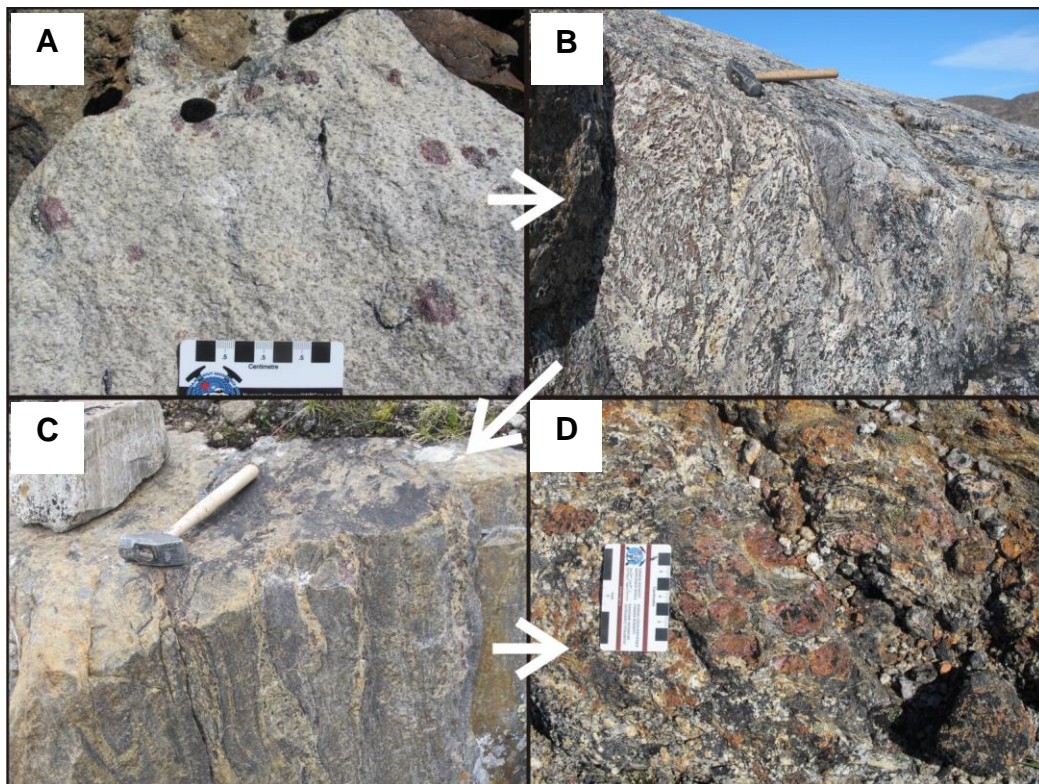

Figure 2.2: Field photos from the western domain of Hall Peninsula showing the gradual transition from garnet-leucogranite (A) to migmatitic pelite (B, C) to pelite (D). Hammer is 40 cm in length, wooden handle points north. Scale card is in centimetres.

FIELD METHODS

The two study areas on either side of Newton Fiord were chosen for this project based on several factors. The eastern lithological domain of Hall Peninsula, which contains both Archean and Paleoproterozoic metasedimentary rocks, was ruled out in order to avoid the complications of inherited phases of Archean deformation and metamorphism. Based on the ages obtained by Scott (1999), the western domain contains only Paleoproterozoic rocks and therefore the deformation can be constrained to the Trans-Hudson Orogeny. The close proximity of the two sites allows for a direct comparison of the structures on the limb of a regional fold versus the structures and mineral assemblages within the hinge of a regional fold.

Twenty-two samples were collected, distributed approximately evenly between Sillimanite Ridge and Barrow Peninsula. A representative sample was taken for each lithology at both locations. The remaining samples targeted pelite with large porphyroblasts, in an effort to find preserved fabrics of an earlier generation. Wherever possible, samples were oriented in the field.

For petrographic analysis, samples were cut both parallel and perpendicular to the regional lineation that is defined by sillimanite and is generally parallel to fold hinges. Where this lineation was poorly developed, the samples were cut either parallel or perpendicular to the dominant foliation.

BARROW PENINSULA

The Barrow Peninsula study area is located on the western side of Newton Fiord and lies within the hinge zone of a regional fold (Figs. 2.1 and 2.3). It consists of interbedded pelite, semipelite and psammite with minor calc-silicate lenses that are cut by orthopyroxene-bearing monzogranite and all of which are crosscut by leucocratic garnet-bearing monzogranite (Fig. 2.3).
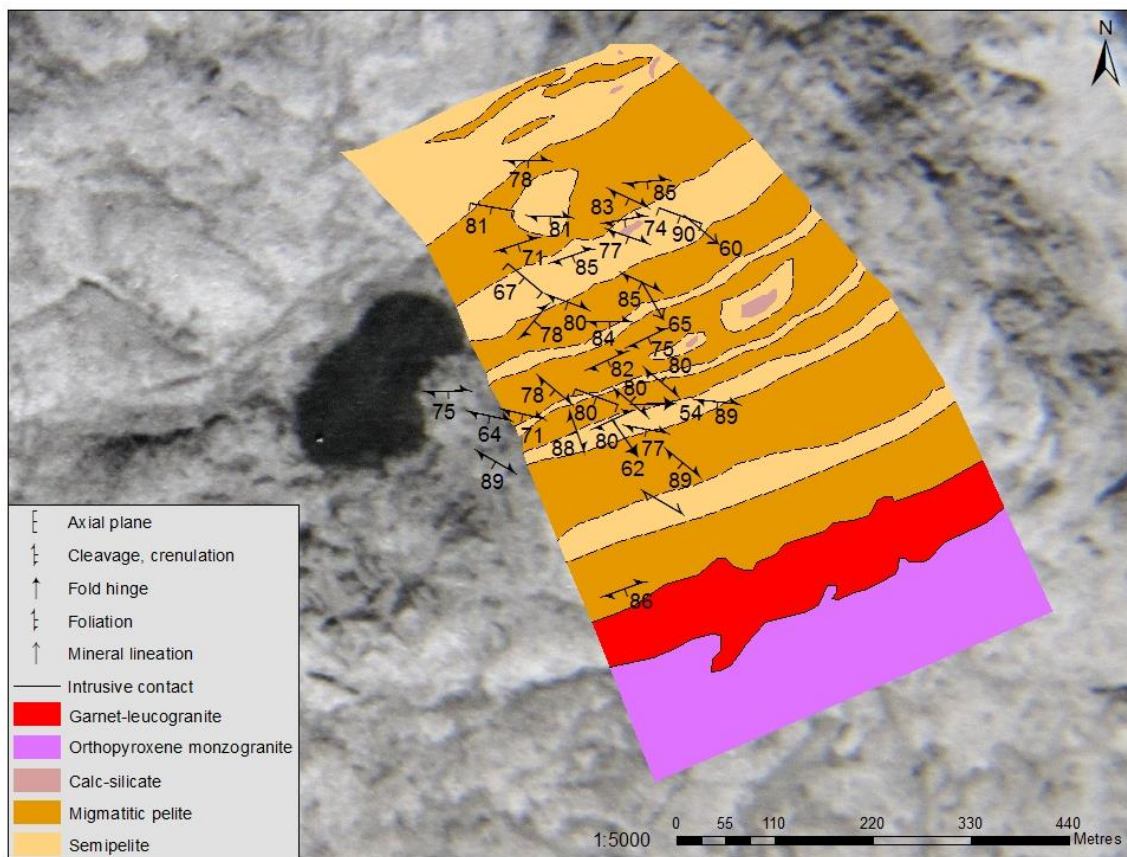

Figure 2.3: Geological map of western study area, Barrow Peninsula, superimposed on a geo-referenced airphoto. See Figure 2.1 for location in the Newton Fiord region.

Pelite & Psammite

The dominant lithology at Barrow Peninsula is migmatite, interpreted to represent pervasively melted pelite and psammite. The psammite is more refractory and is preserved as rafts within the melted pelite (Fig. 2.4A). Garnet crystals are generally dark red to purple and generally between 2-3 cm in diameter. The sillimanite is prismatic and coarse-grained.

In thin section the pelite has a mineral assemblage of garnet + sillimanite + cordierite + biotite + K-feldspar + plagioclase + quartz + melt +/- ilmenite +/- spinel +/- rutile (Fig. 2.4B). The textural relationships and mineral assemblages related to multiple metamorphic events are presented in chapter 3.

Graphitic semipelite

The graphitic semipelite is a marker bed that can be traced around the regional fold in Newton Fiord (Fig. 2.1). In the field graphite is relatively abundant, dark gray and occurs as mats or is disseminated throughout the semipelite unit (Fig. 2.4C).

In thin section the graphitic semipelite has a mineral assemblage of garnet + biotite + sillimanite + cordierite + plagioclase + graphite + K-feldspar + quartz + rutile +/- orthopyroxene +/- spinel (Fig. 2.4D). Graphite is present as opaque, randomly oriented laths scattered throughout the matrix.

Charnockite

The charnockite is recognized in the field by characteristic greasy-green plagioclase and orthopyroxene phenocrysts (Fig. 2.4E). Garnet is present only where the
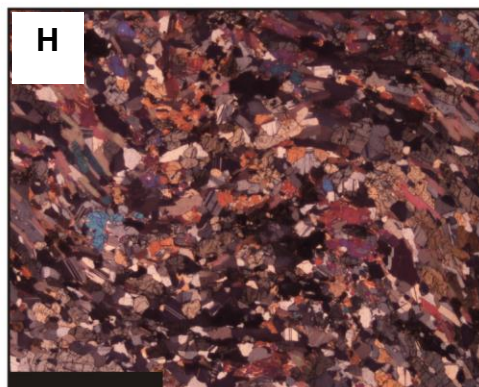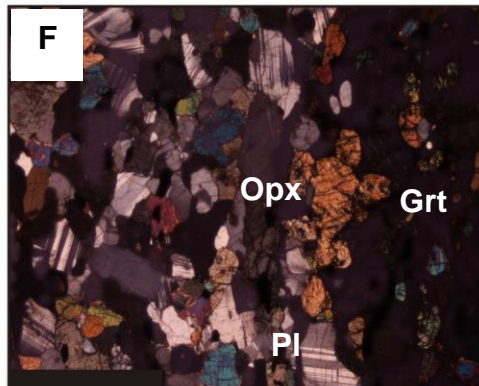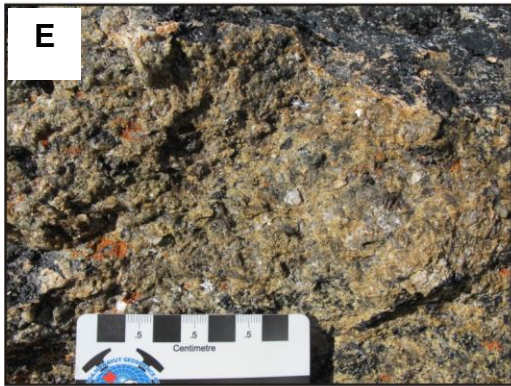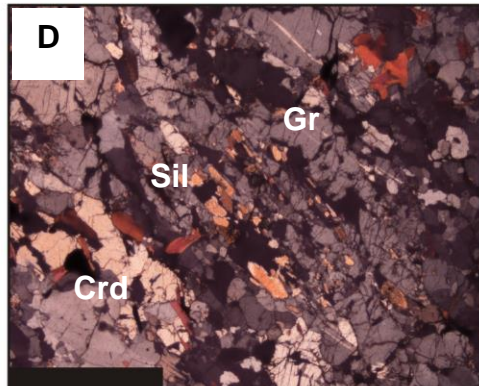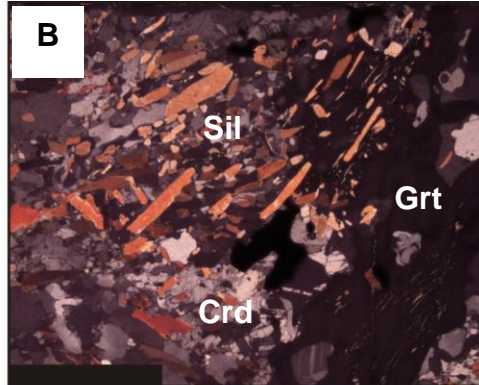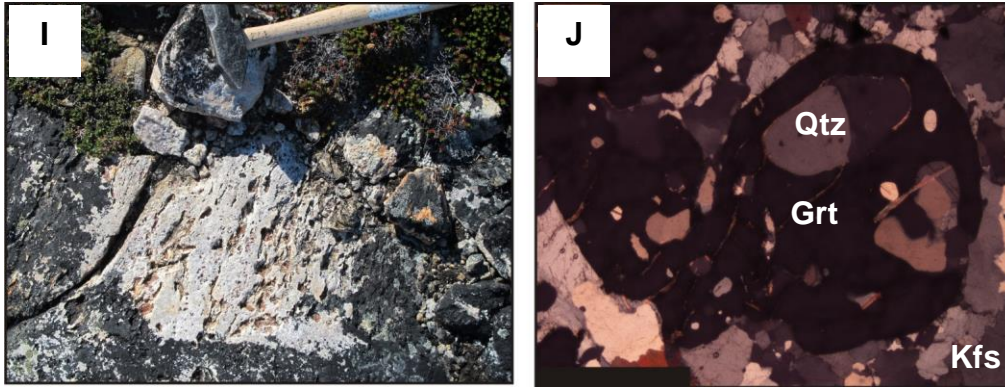
Figure 2.4: Barrow Peninsula lithologies. (A) Field photo of migmatitic pelite, a raft of psammite is outlined in a black, dashed line. (B) Representative photomicrograph of migmatitic pelite. (C) Field photo of graphitic semipelite. (D) Representative photomicrograph of graphitic semipelite. (E) Field photo of charnockite showing greasy-green plagioclase and orthopyroxene phenocrysts. (F) Representative photomicrograph of charnockite. (G) Field photo of minor calc-silicate nodule, which is outline in a black, dashed line. (H) Representative photomicrograph of calc-silicate nodule. (I) Field photo of garnet-leucogranite. (J) Representative photomicrograph of garnet-leucogranite. Hammer is 40 cm in length, wooden handle points north. Scale card is in centimetres. Scale bar on photomicrographs is 2 mm.

charnockite intruded garnet-bearing metasedimentary rocks. The charnockite is restricted along the southern part of the Barrow Peninsula map area and is in sharp contact with garnet-leucogranite. It is moderately to strongly foliated. Outside of the map area further to the north and south, massive to weakly foliated charnockite is the dominant rock type with rafts of metasedimentary rocks.

In thin section the charnockite has a mineral assemblage of orthopyroxene + biotite + plagioclase + quartz +/- garnet +/- ilmenite (Fig. 2.4F).

Garnet-leucogranite

The garnet-leucogranite crosscuts all other units at Barrow Peninsula and is spatially associated with the migmatitic pelite unit (Figs. 2.3). It is relatively fine grained, with garnets greater than or equal to 0.5 cm in diameter (Fig. 2.4G). The garnets are lilac-purple and the quartz is typically glassy-gray to pale blue. The thickest garnet-leucogranite unit occurs in the southern Barrow Peninsula map area and clearly cross-cuts the foliated charnockite. Elongate quartz grains define a weakly developed foliation in the garnet-leucogranite.

In thin section the garnet-leucogranite has a mineral assemblage of garnet + quartz + K-feldspar + plagioclase +/- biotite and the quartz typically includes fine needles of rutile (Fig. 2.4H).

Calc-silicate nodules

The calc-slicate nodules are a minor lithology present only as rafts within the migmatite, semi-pelite, and garnet leucogranite units at Barrow Peninsula. The lenses of calc-silicate range in size from 0.3 to 4 m in length and biotite is typically golden-brown (Fig. 2.4I).

In thin section the calc-silicate has a mineral assemblage of clinopyroxene + plagioclase + biotite + quartz (Fig. 2.4J).

SILLIMANITE RIDGE

The Sillimanite Ridge study area is located on the eastern side of Newton Fiord and lies on the limb of a regional fold (refer to Fig. 2.1 for location). It consists primarily of

interbedded pelite and psammite (Fig. 2.5). The oldest metaplutonic unit is an orange-weathering charnockite with greasy green plagioclase and garnet where in contact with the metasediment. The charnockite is exposed at the western end of the Sillimanite ridge area but also forms as minor bedding-parallel sheets within the pelite and psammite. All rocks are cut by a white-weathering garnet-leucogranite with distinctive lilac-coloured garnet and glassy gray quartz.
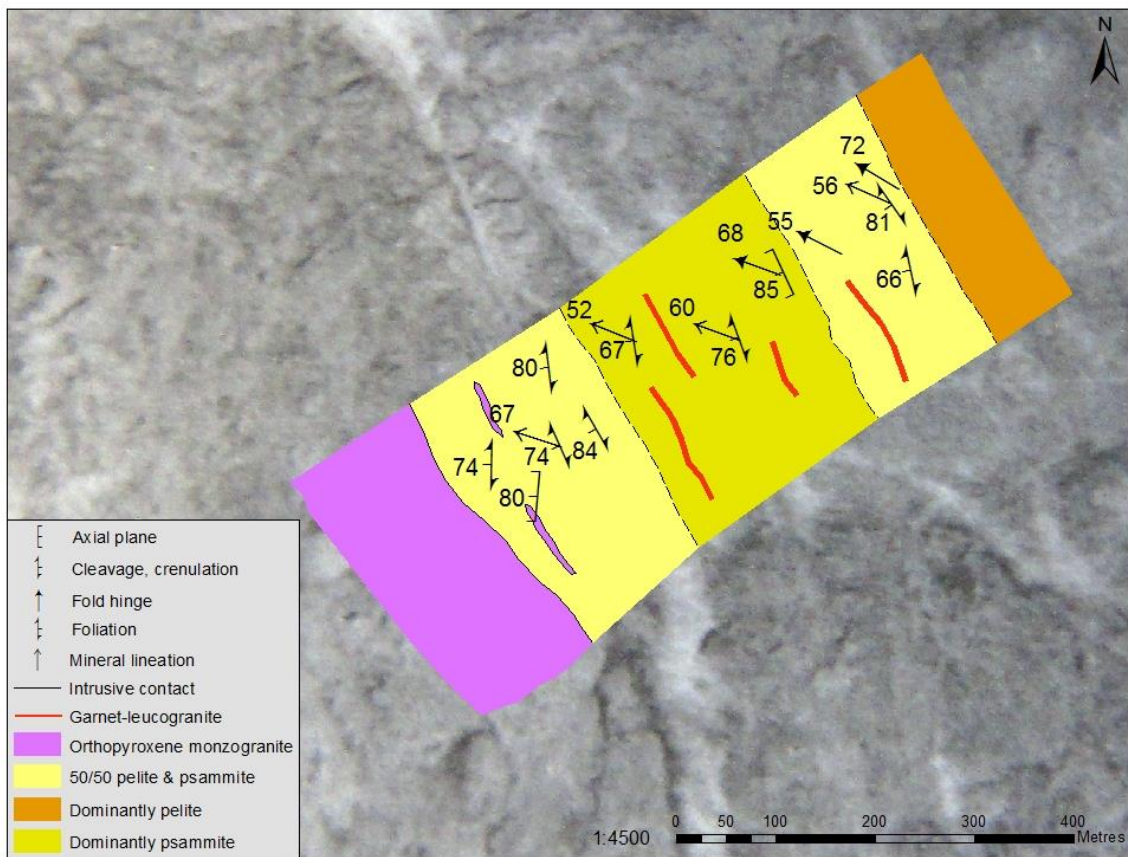
Figure 2.5: Geological map of eastern study area, Sillimanite Ridge, superimposed on a geo-referenced airphoto.

Pelite & Psammite

Pelite and psammite are commonly interbedded throughout this area; pelite is recognized by an abundance of biotite and aluminosilicates whereas the psammite is quartz-rich. Bedding is recognized where garnet-biotite-rich pelite is interbedded with quartz-rich psammite (Fig. 2.6C). Generally individual beds range from 5 to 20 cm and cryptic cross bedding and graded bedding are rarely preserved.

In the pelite garnet crystals can be as large as 8 cm in diameter in the field, though on average most grains are approximately 2 cm in diameter, and are generally dark reddish-purple. Sillimanite is coarsely crystalline, strongly aligned and extremely abundant (Fig. 2.6A).

In thin section the pelite has a mineral assemblage of garnet + sillimanite + biotite + K-feldspar + cordierite + plagioclase +/- ilmenite +/- spinel +/- rutile (Fig. 2.6B). In the psammite, garnet crystals are generally well rounded and between 2-3 cm in diameter. Prismatic sillimanite is associated with garnet between more quartz-rich zones (Fig. 2.6C). In thin section the psammite has a mineral assemblage of garnet + sillimanite + K-feldspar + quartz + plagioclase + biotite (Fig. 2.6D).

Charnockite

This magmatic orthopyroxene-bearing monzogranite is part of the same regional lithology as the one present at Barrow Peninsula (Fig. 2.6E). This unit is orange weathering and contains distinctive "greasy-green" plagioclase (Fig. 2.6E). Garnet is

only present where the charnockite has intruded garnet-bearing metasedimentary rocks

Orthopyroxene phenocrysts are dark brown, euhedral and average 1-2 cm in length.

Figure 2.6 (next page): Sillimanite Ridge lithologies. (A) Field photo of pelite. (B) Representative photomicrograph of pelite. (C) Field photo of psammite. (D) Representative photomicrograph of psammite. (E) Field photo of charnockite showing orthopyroxene phenocrysts. (F) Representative photomicrograph of charnockite. (G) Field photo of garnet-leucogranite. (H) Representative photomicrograph of garnet-leucogranite. Hammer is 40 cm in length, wooden handle points north. Scale card is in centimetres. Scale bar on photomicrographs is 2 mm.
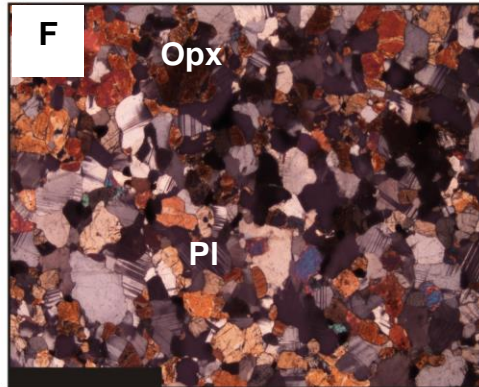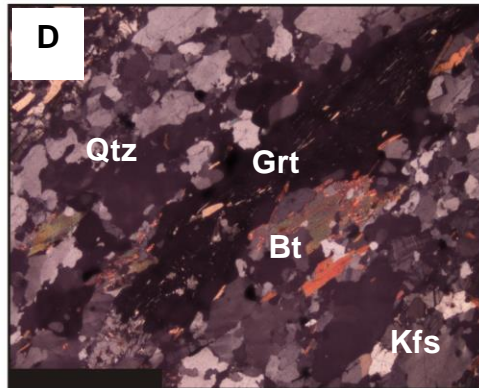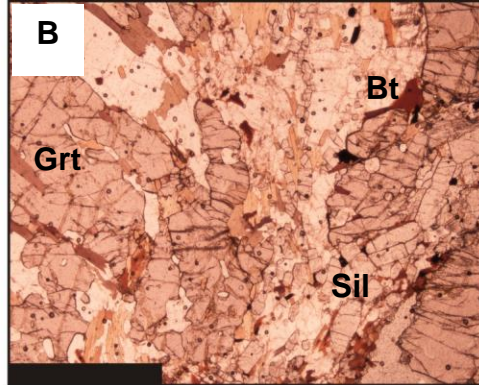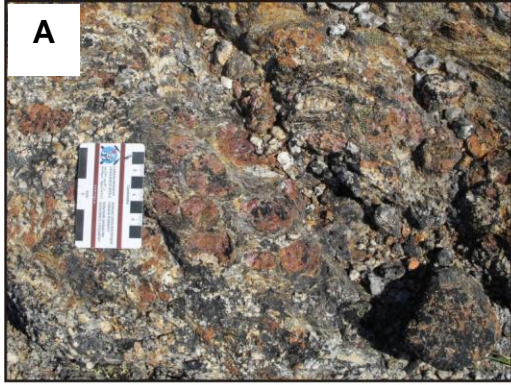
In thin section the charnockite has a mineral assemblage of orthopyroxene + biotite + plagioclase + quartz +/- garnet +/- ilmenite (Fig. 2.6F).

Garnet-Leucogranite

The garnet-leucogranite occurs both parallel to bedding and crosscuts all other units (Fig. 2.6G). In contrast to Barrow Peninsula, the garnet-leucogranite at Sillimanite Ridge is strongly deformed and is generally boudinaged on the limbs of minor folds. Garnet is pale lilac purple and much smaller than in the other units; generally with a diameter less than 1 cm. Quartz is relatively coarse-grained and is distinctly glassy gray.

In thin section the garnet-leucogranite has a mineral assemblage of garnet + quartz + K-feldspar + plagioclase (Fig. 2.6H).

STRUCTURE

At Barrow Peninsula, the cleavage domains are between 10-15 cm apart and are steeply southwest-dipping; the intervening microlithons are subparallel to the cleavage domains and are steeply southeast-dipping (Fig. 2.7). This spaced foliation only occurs in the hinges of regional folds, where pre-existing fabric elements were shielded from some of the shear strain experienced on the limbs during folding. The orientation of the subparallel microlithons likely represents the orientation of a fabric that developed prior to regional folding.

Figure 2.7: field photo of spaced foliation at Barrow Peninsula. The bottom photo (B) is annotated to show cleavage domains and orientation of intervening microlithons. Hammer is 40 cm in length, wooden handle points north.

The tectonic fabric elements at Sillimanite Ridge are strong, penetrative, and west-dipping. By comparison, the fabrics elements at Barrow Peninsula are variably developed and either southeast- or southwest-dipping (Fig.2.8).

The main fabric is a regionally-penetrative bedding-parallel sillimanite-biotite foliation. This fabric is folded and a new axial-planar fabric crenulates the earlier fabric in the hinges of minor folds. Minor folds at Sillimanite Ridge follow the same trend as regional folds and are generally northwest-plunging. Extensional strain along the hinge of folds resulted in a strong, hinge-parallel mineral growth lineation defined by sillimanite. In the hinge of folds, planar elements are generally weaker than linear elements. The consistent orientation of the foliation and lineation at Sillimanite Ridge is characteristic of fold limbs across the western domain of Hall Peninsula. Sillimanite Ridge is characterized by high strain transposition on the limb of a regional fold. Passchier and Trouw (2005) describe transposition as the progressive erasure or re-orientation of an older structure by deformation and/or metamorphic processes. During regional folding, the limbs experienced higher strain and pre-existing fabric elements were rotated into parallelism with the axial plane of the regional fold.

In contrast to the uniformity at Sillimanite Ridge, Barrow Peninsula has planar and linear fabric elements that vary in orientation and intensity. The foliation is spaced with two distinct orientations and the lineation is generally poorly developed. At Barrow, the cleavage domains are 10-15 cm apart and are steeply southwest-dipping; the intervening microlithons are subparallel to the cleavage domains and are steeply southeast-dipping. This spaced foliation is only preserved in the hinges of regional folds, where pre-existing fabric elements were shielded from some of the shear strain

experienced on the limbs during folding. The orientation of the subparallel microlithons likely represents the orientation of a fabric that developed prior to regional folding.
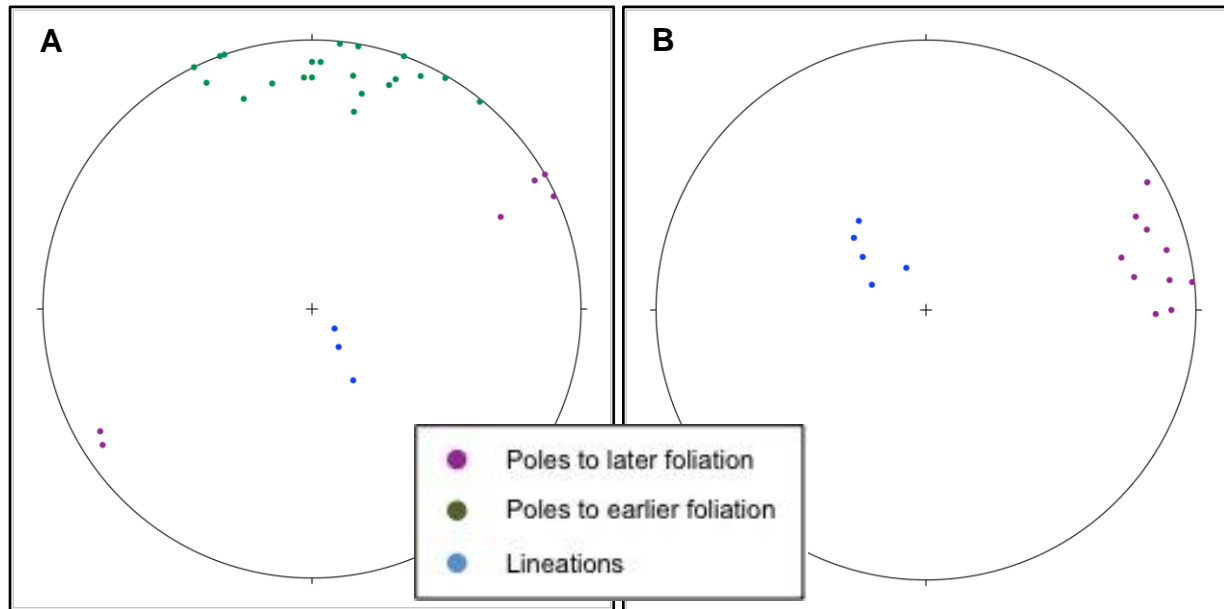
Figure 2.8: Equal area stereonet plots foliation and lineation measurements from Barrow Peninsula (A) and Sillimanite Ridge (B). In the hinge of a regional fold, Barrow Peninsula was shielded from some of the higher strain transposition attributed to regional folding and provides a window into earlier deformation. This resulted in the preservation of older fabric elements, represented by the green poles to foliation on plot (A). Sillimanite Ridge experienced nearly complete transposition or re-orientation of pre-existing fabric elements.

Chapter 3: Relative chronology of mineral-fabric relationships

INTRODUCTION

Extensive petrography has revealed three distinct generations of tectonic fabric elements present in the Newton Fiord region. The fabrics are particularly well illustrated by different generations of sillimanite growth based on textural relationships. The earliest fabric is defined by fibrolitic sillimanite preserved in the core of garnet porphyroblasts and only recognized in thin section. Inclusion trails of early sillimanite range from randomly orientated to strongly aligned and generally occur at a high angle to the dominant external foliation. The second fabric is defined by strongly planar-aligned medium-grained sillimanite in the rims and strain shadows of garnet porphyroblasts as well as the dominant gneissosity recognized in the field. The third fabric is a dominantly linear fabric and is defined by the extremely coarse matrix sillimanite that wraps garnet porphyroblasts and is aligned parallel to the regional lineation.

These fabrics have been divided into an early phase of deformation and a late, progressive deformation including the main regional foliation and east-verging folds with associated hinge-parallel extension. Metamorphic mineral growth has been categorised into metamorphic events based on textural relationships relative to the three dominant fabrics. Figure 3.1 outlines the nomenclature used to describe the relative chronology of metamorphic events and deformation phases throughout this thesis.
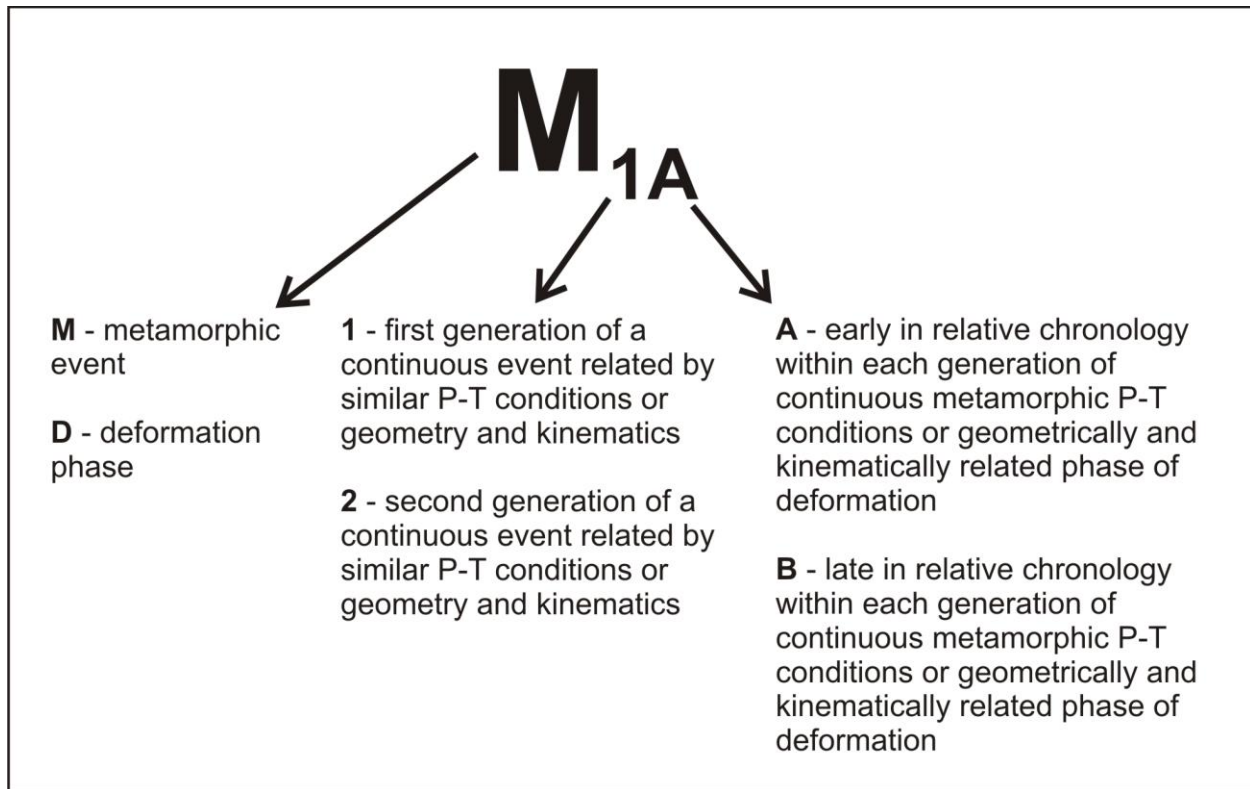
Figure 3.1: Explanation of abbreviations used to describe the chronology of metamorphism and deformation throughout this thesis.

Linked field observations and petrographic analysis have revealed two main tectonometamorphic events, D_1 and D_2, each of which can be further characterized based on relative chronology of mineral growth and fabric formation. The first event D_1/M_{1A} refers to a flattening fabric formed at granulite facies conditions and M_{1B} refers to an associated partial melt phase. The second event, D_2/M_2, is a progressive deformation and associated metamorphism that began with the main regional fabric-forming phase (D_{2A}/M_{2A}) at upper amphibolite to lower granulite facies conditions followed by a phase of folding and associated shearing of fold limbs (D_{2B}/M_{2B}), also at upper amphibolite to lower granulite facies conditions.

Migmatitic pelite from Sillimanite Ridge and Barrow Peninsula were chosen for detailed petrography based on their comparable mineral assemblages and porphyroblastic

texture. The graphitic semipelite was purposefully omitted to avoid the unnecessary complications presented by a CO_2 vapour phase. Metamorphic orthopyroxene can be quite important in determining relative pressure-temperature conditions; however the presence of graphite, which contains carbon, significantly complicates pressure-temperature estimates. When CO_2 is present as the vapour phase rather than H_2O, the stability fields in a pressure-temperature diagram change (Yardley, 1989). For this reason, all further pressure-temperature interpretations have been based on the pelite and migmatite units, in which it can be reasonably assumed that H_2O is the only vapour phase present, if a free fluid phase is present at all. Below is a description of the data collected for each phase of deformation and metamorphism.

D_1/M_{1A}

The first event, D_1/M_1, is characterized by weakly to strongly aligned fine- to medium-grained sillimanite (M_{1A}) that is only preserved as inclusion trails in garnet and cordierite porphyroblasts, followed by voluminous garnet-cordierite-bearing leucosome formation (M_{1B}). M_1 has been subdivided to represent metamorphism concurrent with D_1 deformation (M_{1A}) and the heat of metamorphism outlasting D_1 deformation (M_{1B}).

Within the pelitic rocks, the M_{1A} assemblage is only preserved in garnet porphyroblasts and consists of garnet + sillimanite + K-feldspar + ilmenite + cordierite + quartz +/- rutile. The cores of garnet porphyroblasts that are largely free of biotite inclusions contain fine fibrolitic sillimanite needles. The fibrolite is variably aligned, with a "starburst" shape that suggest M_{1A} sillimanite wrapped earlier garnet porphyroblasts (Fig 3.2A, B). Multiple generations of porphyroblast growth resulted in complex inclusion trail patterns. As a

result, evidence for the earliest phase of deformation is cryptic. In a few samples, garnet porphyroblasts may have rotated during fabric development, producing sigmoidal inclusion trails (Fig. 3.2C, D). Alternatively, the sigmoidal inclusion trail may be a result of early fabric development followed by crenulation and subsequent porphyroblast overgrowth. In either case, the inclusion trail in this and other porphyroblasts are at a high angle to the external S_{2A} foliation (Fig. 3.2C, D).
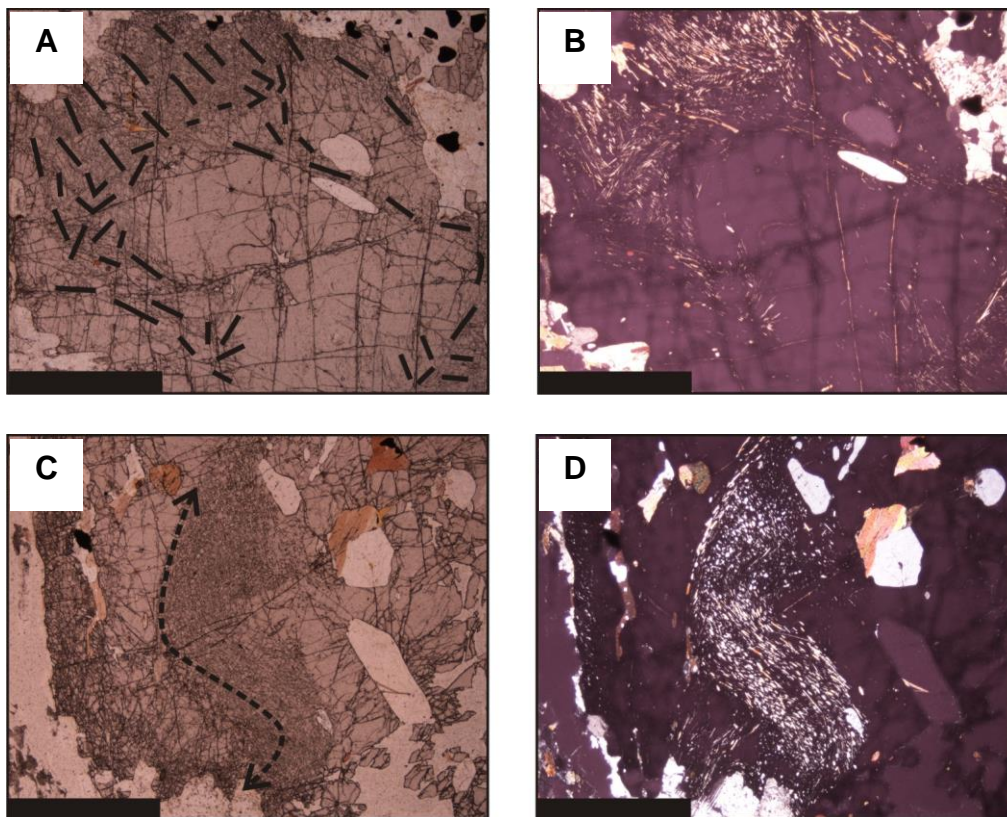
Figure 3.2: (A) & (B) Photomicrographs of "starburst" pattern of sillimanite inclusions in garnet porphyroblasts. (C) & (D) Photomicrographs of sigmoidal sillimanite inclusion trail in a garnet porphyroblast possibly produced from porphyroblast rotation during fabric development. Scale bar is 2 mm. Photomicrographs (A) & (C) were taken in plane polarized light and photomicrographs (B) & (D) were taken in crossed polarizes light.

A sample from the migmatite unit at Barrow Peninsula cut parallel to the L_{2B} lineation contains a portion of the leucosome and a portion of the mesosome, in which there are

several generations of garnet porphyroblasts (Fig. 3.3). Some of the early garnet porphyroblasts contain fibrolitic sillimanite inclusion trails at a high angle to the S_{2A} foliation (Fig 3.3A, B, C, D). There is an inclusion-free core of garnet at the centre of these sillimanite inclusions suggesting that the sillimanite that defines the earliest D_1 fabric may have wrapped around earlier porphyroblasts. Garnet porphyroblasts with D_1 sillimanite inclusion trails are commonly free of biotite inclusions.
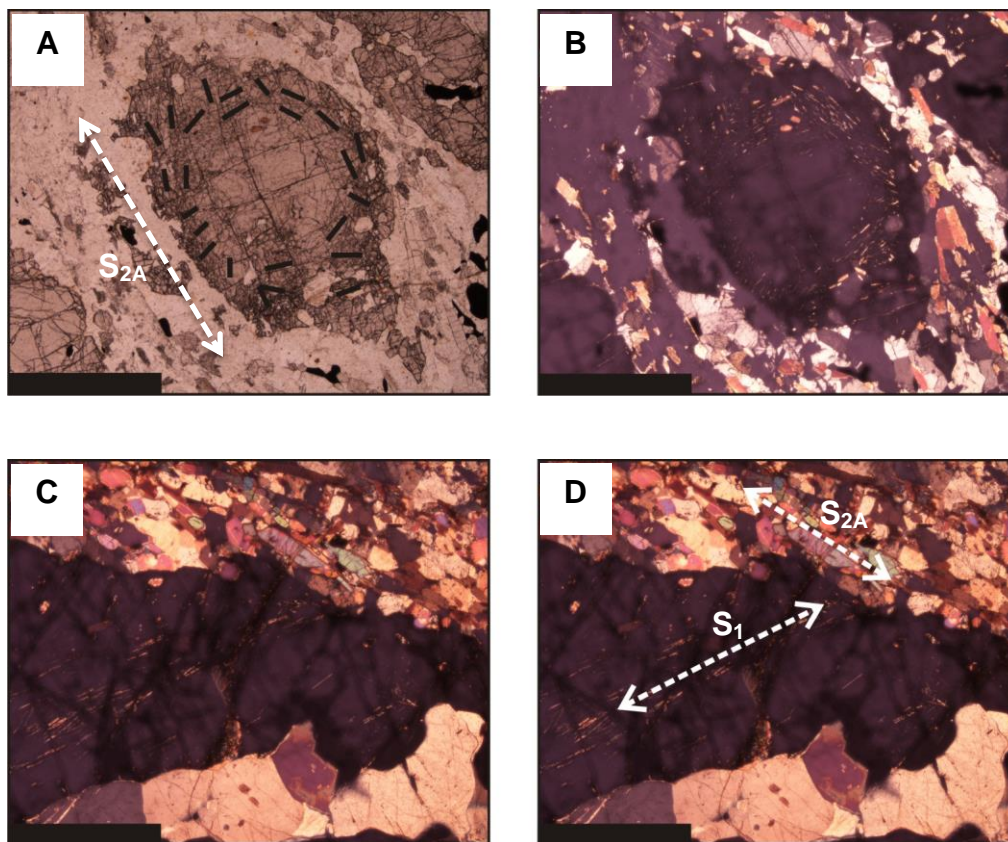
Figure 3.3: Photomicrographs of S_1 sillimanite inclusion trails in garnet porphyroblasts at a high angle to the external matrix fabric. Scale bar is 2 mm. Photomicrograph (A) was taken in plane polarized light and photomicrographs (B), (C) & (D) were taken in crossed polarized light.

Cordierite and K-feldspar also preserve rare fibrolite inclusions. Inclusions of green spinel in several garnet porphyroblasts and pale green and brown spinel inclusions in

coarse matrix sillimanite also suggest a high temperature metamorphic event; however the generation of garnet porphyroblasts that contain these inclusions is unclear. Spinel is included in the core of porphyroblasts that contain fibrolitic sillimanite inclusions as well as in the core of porphyroblasts that are sillimanite-free (Fig 3.4A, B).
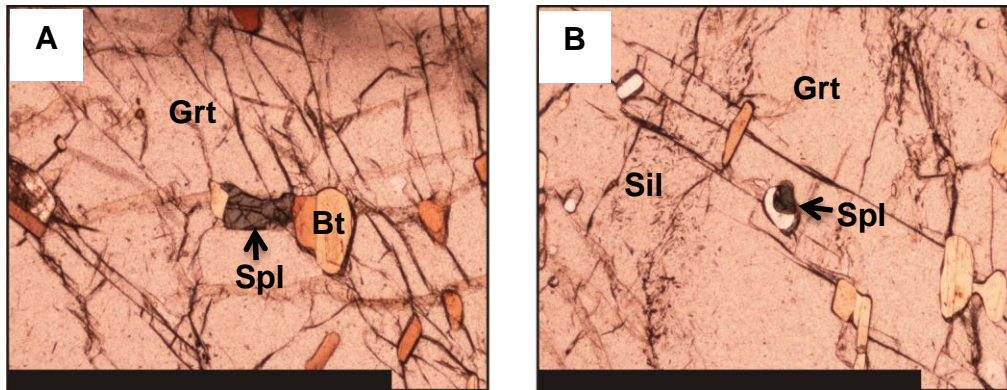
Figure 3.4: (A) Photomicrographs of green spinel inclusion in a garnet porphyroblasts that is free of sillimanite inclusions. (B) Photomicrograph of green spinel inclusion in a garnet porphyroblast that contains fibrolitic sillimanite inclusions. Scale bar is 2 mm.

Both the Paleoproterozoic metasedimentary rocks and the charnockite were affected by D_1 deformation, which resulted in a variably developed foliation oriented approximately north-northeast. In the field, the metasedimentary rocks and the charnockite are both cut by a garnet-leucogranite that displays only late deformation structures.

M$_{1B}$

The M$_{1B}$ leucosome is related to the garnet-leucogranite in the field. The garnet-leucogranite crosscuts all other units and is spatially associated with the migmatite and the pelite (Fig. 3.5A, B). The M$_{1B}$ assemblage consists of plagioclase + cordierite + K-feldspar + quartz +/- garnet +/- sillimanite. It is considered distinct from M$_{1A}$ because

M_{1B} mineral growth overlapped and slightly outlasted M_{1A} mineral growth; this is evident where M_{1B} mineral phases overgrow M_{1A} mineral phases (Fig. 3.7B).
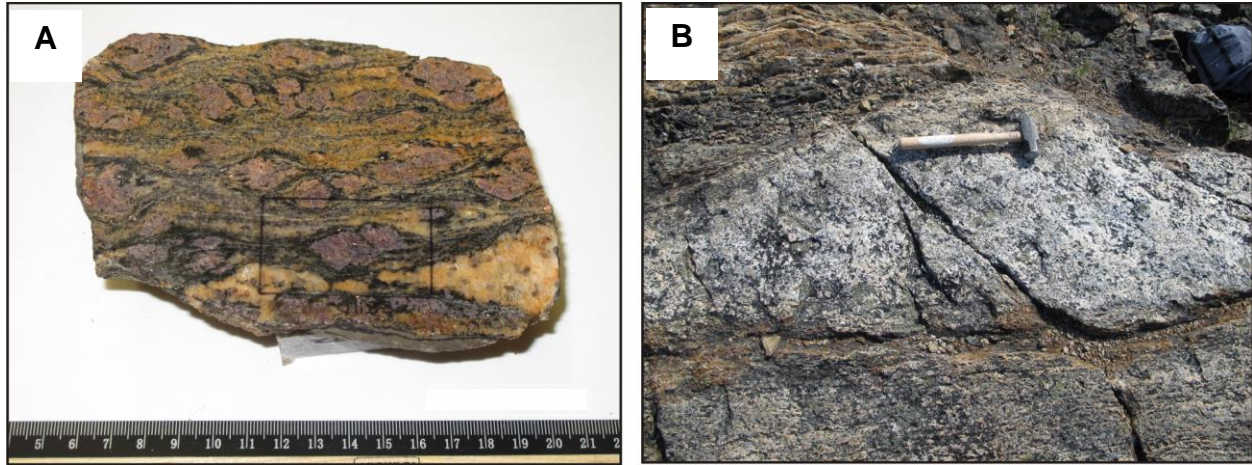
Figure 3.5: (A) Slab photo of a pelite from Sillimanite Ridge showing both mesosome and leucosome phases (A - ruler is in centimetres). (B) Field photo of leucosome spatially associated with and crosscutting the pelite (B - hammer is 40 cm in length).

Large knots of K-feldspar porphyroblasts (up to 7 mm) display abundant exsolution lamellae and are generally perthitic microcline. Quartz grains range from a granoblastic polygonal texture to having irregular, sutured grain boundaries and significant undulose extinction (Fig.3.6A, B).
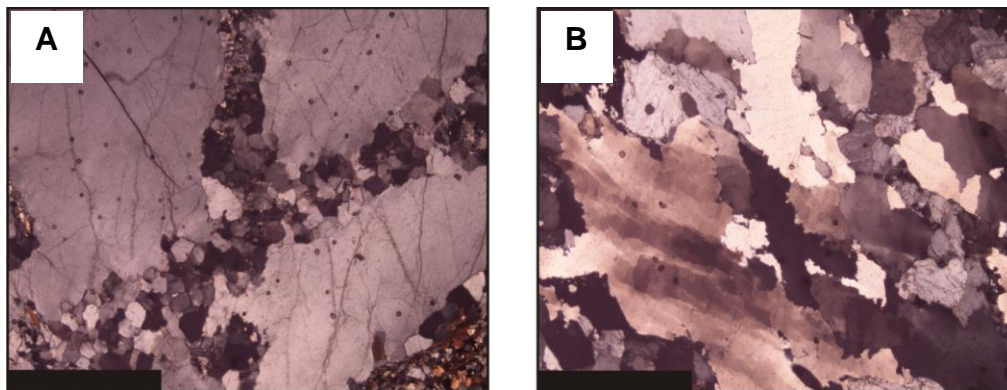
Figure 3.6: Photomicrograph showing large knot of K-feldspar (A). Photomicrograph showing quartz grains with sutured grain boundaries and undulose extinction (B). Scale bar is 2mm.

Cordierite is spatially associated with the leucosome and is most abundant along the the leucosome and the mesosome contact. Cordierite has deformed flame twinning and is rarely in equilibrium with the surrounding matrix (Fig. 3.7A). In particular, cordierite embays and overprints garnet porphyroblasts containing aligned M_{1A} sillimanite inclusion trails (Fig. 3.7B). Occasionally cordierite contains fine sillimanite inclusions.
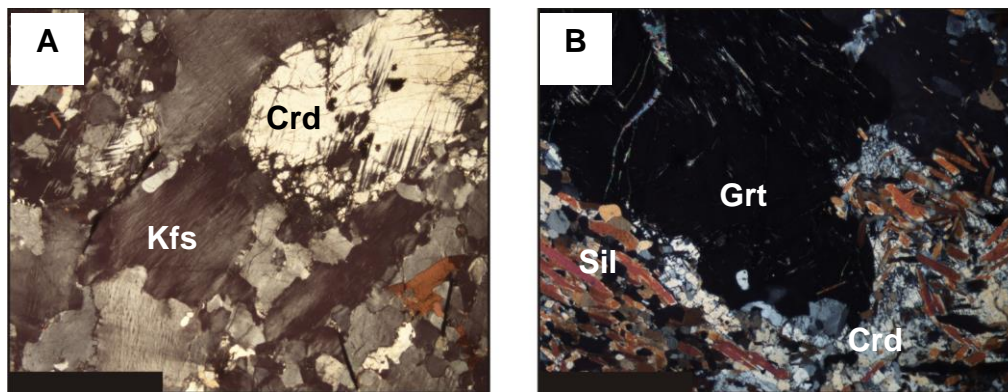
Figure 3.7: (A) Photomicrograph showing cordierite with flame twinning. (B) Photomicrograph showing corderite embaying a garnet porphyroblast and being overprinted by coarse matrix sillimanite. Scale bar is 2mm.

Idioblastic to subidioblastic garnet porphyroblasts contain large rounded inclusions of quartz, plagioclase, and K-feldspar that are surrounded by melt films (Fig. 3.8). These porphyroblasts likely grew within the leucosomlle at the time of melt crystallization, suggesting a peraluminous melt phase. Garnet and cordierite are the only iron- and magnesium-bearing phases in equilibrium with the leucosome. Biotite tends to occur as large mats, which overgrow garnet and cordierite. Texturally, biotite is not in equilibrium with other leucosome phases, it is a later fabric forming mineral; however some biotite may also have formed from rehydration during melt crystallization.
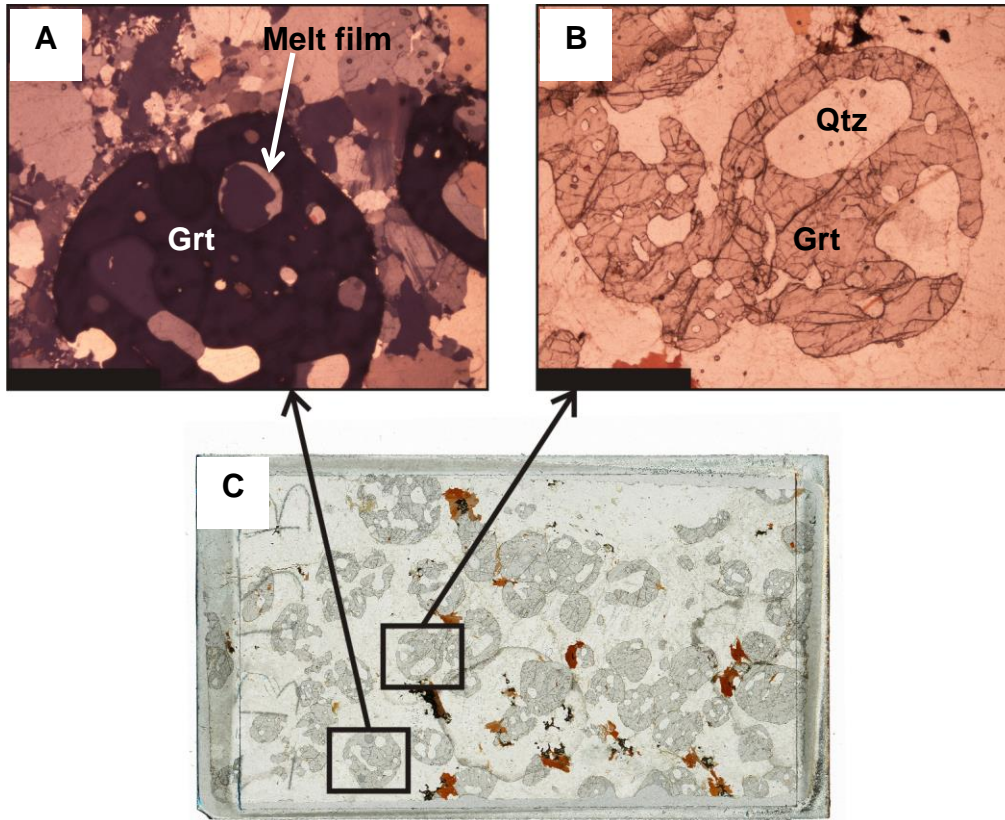
Figure 3.8: (C) Thin section scan showing abundant garnet porphyroblasts in the leucosome. Biotite overgrows garnet and cordierite and is attributed to M_2. (A) Photomicrograph of a garnet porphyroblast containing a K-feldspar inclusion surrounded by a melt film. (B) Photomicrograph of garnet porphyroblast in the leucosome. Scale bar on photomicrographs is 2mm. Thin section is 4.5 cm x 2.5 cm.

At both Sillimanite Ridge and Barrow Peninsula, the foliated charnockite, which crosscuts the pelitic units, is cut by the garnet-leucogranite. This garnet-leucogranite does not show any indication of an early fabric, except where it has entrained a portion of the mesosome. Hence, the melting is attributed to M_{1B} which post-dates D_{1A} fabric development.

Summary of D_1/M_1

Table 3.1 summarizes D_1 deformation and associated M_1 metamorphism. Aligned sillimanite inclusion trails that are at a high angle to the matrix foliation provide evidence for an early fabric that pre-dated the main regional deformation. The rare sigmoidal inclusion trails may be attributed to porphyroblast rotation (Passchier et al., 1992) or to porphyroblast growth over a previously crenulated fabric (Bell et al., 1992). The inclusion trails that are at a high angle to the external foliation in some samples indicate that this fabric is distinct from and earlier than the matrix foliation.

The distinct absence of biotite in conjunction with the presence of abundant cordierite suggest that M_1 equilibration may have occurred at granulite conditions, most likely above the biotite dehydration melting reaction line ("biotite-out"). The biotite that is present in the matrix is likely a later overprint. The euhedral garnets in the leucosome do not show any indication of having grown during a period of significant strain. Therefore it is probable that M_{1B} marginally outlasted D_1 deformation.

Deformation	Metamorphism	Assemblage	Description
D_1	M_{1A}	Grt + Sil + Crd + Kfs + Il + Qtz +/- Rt	Variably aligned fibrolitic Sil inclusions, at high angle to matrix foliation
	M_{1B}	Pl + Crd + Kfs + Qtz +/- Grt +/- Sil	Voluminous partial melt phase, no associated fabric

Table 3.1: Summary table of D_1/M_1.

D$_2$/M$_2$

D$_2$ has been subdivided into an initial fabric-forming phase (D$_{2A}$) and a later phase of folding and shearing (D$_{2B}$) that are kinematically related. D$_{2A}$ deformation produced a regionally-penetrative west- to southwest-dipping fabric (S$_{2A}$) that controls the regional map pattern. D$_{2B}$ produced west to southwest-dipping folds that vary in shape from isoclinal to open.

The M$_2$ metamorphic event was pervasive and long-lived and is interpreted to have persisted during both phases of D$_2$ deformation. It has been subdivided into an early phase (M$_{2A}$) and a late phase (M$_{2B}$) based on overprinting relationships.

D$_{2A}$/M$_{2A}$

D$_{2A}$ is expressed as moderately to shallowly west-dipping gneissosity (S$_{2A}$) defined by interlayered leucosome and sillimanite-biotite mesosome. This fabric is the dominant foliation and is parallel to compositional layering. The associated M$_{2A}$ mineral assemblage consists of garnet + sillimanite + biotite + ilmenite + K-feldspar + plagioclase + quartz +/- melt. This period of metamorphic mineral growth occurred at upper amphibolite facies conditions and was synchronous with S$_{2A}$ foliation development.

Oblate garnets contain biotite inclusions that are parallel to the margin of the porphyroblast. These garnet porphyroblasts likely overgrew pre-existing and preferentially aligned biotite grains. These oblate (pancake-shaped) garnet porphyroblasts indicate that a flattening or pure shear strain component was dominant

during some portion of D_2 deformation. Garnet has a strong crystal structure and is difficult to deform once crystallized, therefore to produce large oblate garnet crystals, they had to have grown during a period of significant flattening strain. Figure 3.9 shows two photomicrographs and a thin section scan from the psammite unit at Sillimanite Ridge. There are two generations of garnet present and both are aligned with S_{2A} foliation on the limbs of the F_{2B} fold. There is an oblate garnet porphyroblast, cut so that only the thin elongate portion is visible, that contains sillimanite and biotite inclusion trails. The sample from which this section was taken was cut both parallel and perpendicular to the axial plane of the fold and this revealed the oblate nature of the garnet porphyroblasts. Large rounded porphyrobasts that do not contain sillimanite inclusions represent later M_2 porphyroblasts. These oblate garnets are folded by late F_{2B} folds and therefore the period of dominantly pure shear can be attributed to D_{2A} deformation, after which strain evolved to include a simple shear component as revealed by limb shearing along F_{2B} folds.
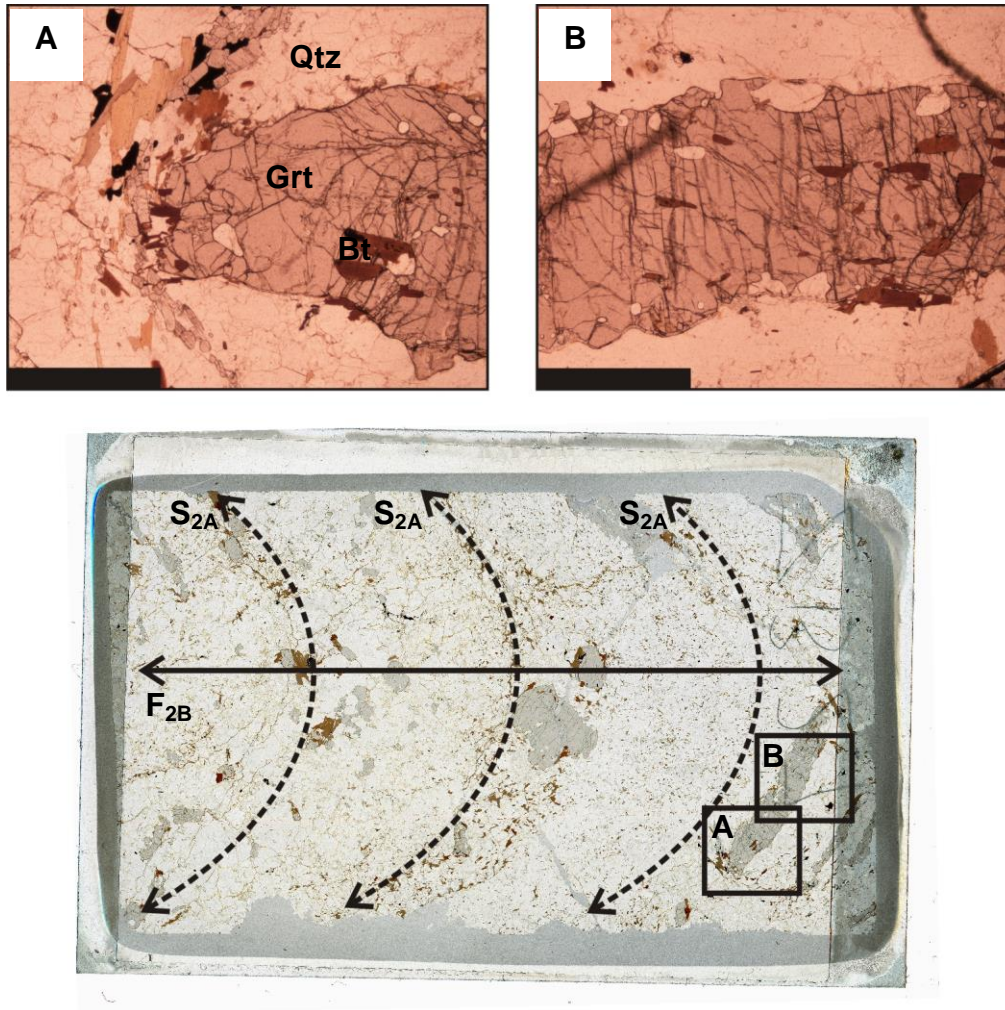
Figure 3.9: Thin section scan and photomicrographs from folded psammite unit at Sillimanite Ridge showing an oblate garnet porphyroblast. Black boxes on the thin section scan indicate location of photomicrographs. Scale bar on photomicrographs is 2 mm. Thin section is 7.5 cm x 5 cm.

Sillimanite defines the foliation and wraps garnet porphyroblasts. These medium-grained sillimanite needles around the rim of garnet porphyroblasts and in the strain shadows of these porphyroblasts represent the second sillimanite growth phase. The second sillimanite also overgrows cordierite within M_{2B} garnet porphyroblasts. Aligned biotite inclusion trails in garnet porphyroblasts (that are free of sillimanite inclusions) are

likely remnants of early M_2 metamorphic mineral growth. Table 3.2 summarizes D_{2A} deformation and the associated M_{2A} metamorphic mineral growth.

Deformation	Metamorphism	Assemblage	Description
D_{2A}	M_{2A}	Grt + Sil + Bt + Kfs + Il + Pl + Qtz +/- melt	West-dipping foliation, main fabric

Table 3.2: Summary table of D_{2A}/M_{2A}.

D_{2B}/M_{2B}

D_2 deformation resulted in moderately west-inclined F_{2B} folds associated with a strong hinge-parallel lineation defined by biotite and very coarse matrix sillimanite (L_{2B}). The accompanying M_{2B} mineral assemblage is the same as M_{2A} and consists of garnet + sillimanite + biotite + ilmenite + K-feldspar + plagioclase + quartz +/- melt.

F_{2B} folds are defined by the folding of the composite $S_0/S_1/S_{2A}$ fabric. Figure 3.10 is a field photo showing an F_{2B} fold of interlayered garnet-leucogranite and pelite. S_{2A}, which has overprinted an earlier S_1 and the original bedding (S_0), is visibly folded by an F_{2B} fold.
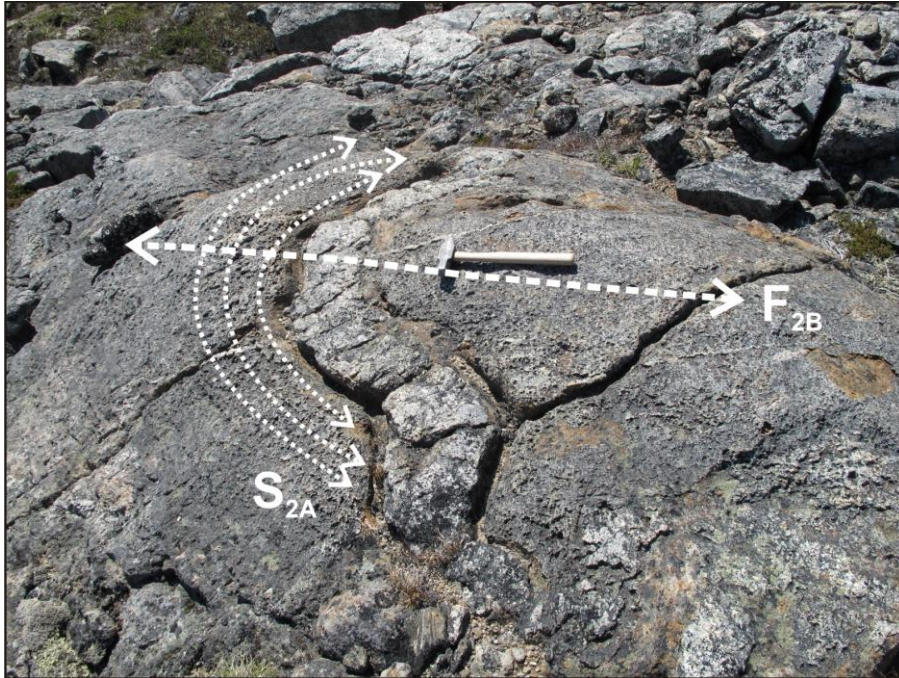
Figure 3.10: Field photo showing an F_{2B} fold folding earlier S_{2A} foliation. Hammer is 40 cm in length, wooden handle points south.

S_{2B} is a weakly developed axial planar foliation defined by biotite and present in the hinge zone of F_{2B} folds. L_{2B} is the dominant fabric element and is a strong hinge-parallel lineation. These rocks are L >> S-tectonites, meaning that the linear (L) fabric element is dominant and the planar (S) fabric element is minor. Figure 3.11 shows photomicrographs and slab photos taken parallel (Fig. 3.11A, C) and perpendicular to the L_{2B} lineation (Fig. 3.11B, D). Biotite and coarse matrix sillimanite define L_{2B} and wrap garnet porphyroblasts. Matrix sillimanite is aligned parallel to L_{2B} and when viewed perpendicular to L_{2B}, the cross sectional area of sillimanite is well displayed.

These petrographic oberservations are consistent with field observations at Barrow Peninsula in which D_{2B} deformation is characterized by open to close folds associated

with a spaced and variably developed axial-planar S_2 foliation and a sillimanite-defined lineation in F_2 hinges. The spaced S_{2B} foliation occurs in narrow (2–3 cm) bands spaced approximately 10-15 cm apart (Fig 2.7). This localized S_{2B} planar fabric is interpreted as shear related within the hinges and on the limbs of F_2 folds.
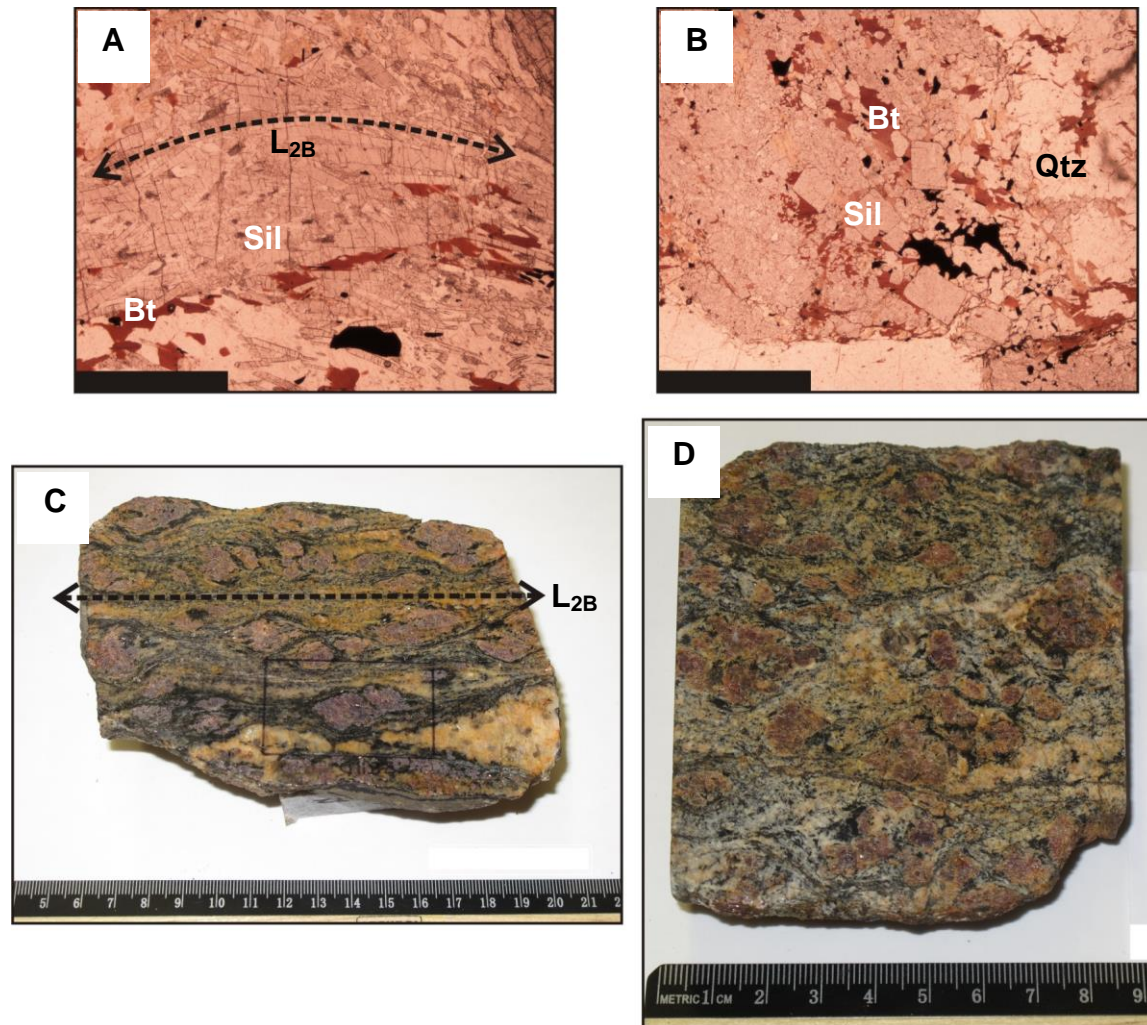
Figure 3.11: Photomicrographs from samples cut parallel (A) and perpendicular (B) to L_{2B}. Scale bar is 2 mm. Slab photos of a sample that was cut parallel (C) and perpendicular (D) to L_{2B}. Ruler is in centimetres.

Further data supporting a late period of shearing are evident at the microscopic scale. Recrystallized quartz and K-feldspar define shear bands that wrap garnet

porphyroblasts (Fig. 3.12). Voluminous melting took place during M_{1B}, however the temperature remained high enough throughout M_2/D_2 that a late partial melt phase, in smaller proportions, is likely. Late leucosome is only identifiable by undeformed myrmekite that overprints older fabric elements and by melt films around matrix minerals, evidence for late melt, late leucosomes makes up only a minor component of the leucosomes present, Matrix quartz shows variable amounts of strain and recovery, from grain size reduction, sutured grain boundaries, subgrain rotation, and undulose extinction to granoblastic polygonal texture, evidence of advanced annealing.

Figure 3.12: Stitched photomicrographs of shear bands consisting of recrystallized quartz and feldspar wrapping a large garnet porphyroblast, in plane polarized light (A) and crossed polarized light (B).

Transposition of fabric elements due to fold-limb shearing is the latest observed expression of D_2 deformation. This transposition is not penetrative; it is observed in

interspersed zones of high and low strain. A similar strain gradient is preserved at Sillimanite Ridge with minor folds that become progressively more isoclinal towards the western edge of the study area (Fig. 3.13). Sillimanite Ridge has been strongly transposed by this fold-limb shearing and preserves no earlier deformation structures, with the exception of porphyroblast inclusion trails. Within the hinge zone, Barrow Peninsula was shielded from much of this high strain shearing and recorded only narrow D_{2B} shear bands and crenulations.

Figure 3.13: Minor folds at Sillimanite Ridge with varying inter-limb angles from open to isoclinal. Hammer is 40 cm in length, wooden handle points north.

During M_2 there was pervasive coarse mineral growth with abnormally large garnet and sillimanite crystals. It is probable that some component of the system inhibited nucleation to preferentially produce large crystals as opposed to many small crystals. Alternatively this may have involved the coarsening of earlier finer-grained minerals, however the details of these growth kinetics are beyond the scope of this thesis. Figure 3.14 shows the abundance of matted sillimanite crystals in the matrix.
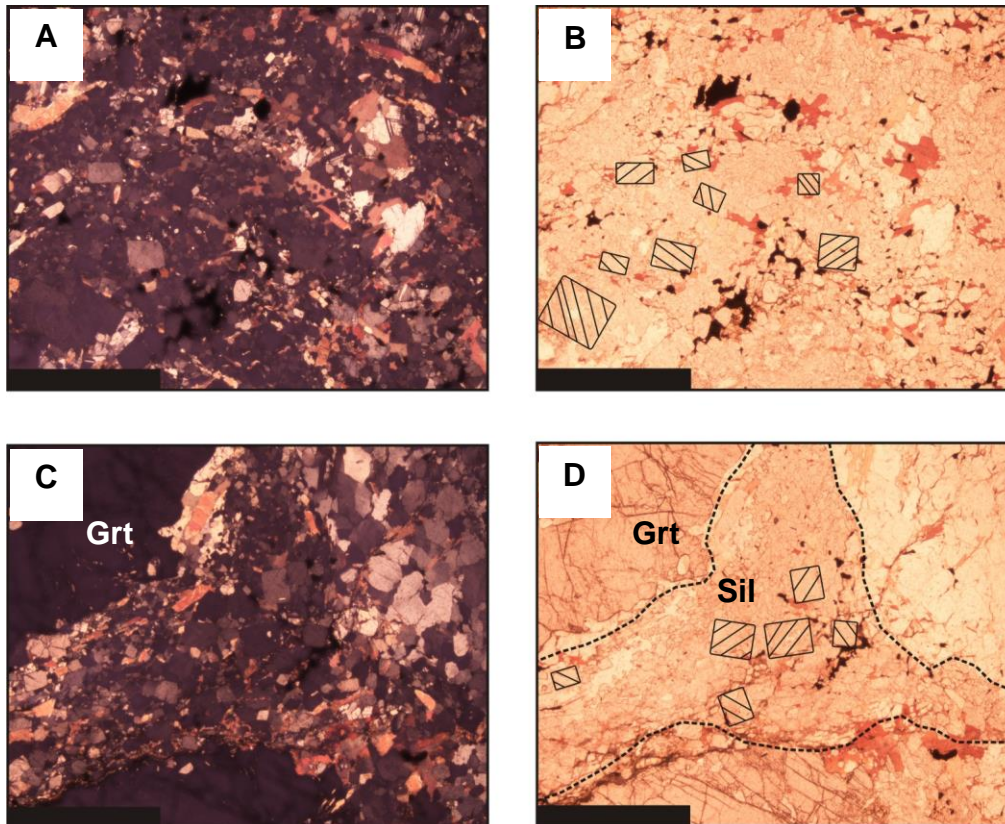
Figure 3.14: Photomicrographs of coarsely matted sillimanite in the matrix, cut perpendicular to the L_{2B} lineation. Scale bar is 2 mm

Garnet porphyroblasts that are sillimanite-free but that contain aligned biotite inclusion trails are part of late M_2 metamorphic mineral assemblage. Garnet porphyroblasts are unusually large (up to 8 cm in the field) and subhedral to euhedral, often embayed by coarse matrix sillimanite. Large patches of biotite grains overprint everything, including garnet porphyroblasts. This biotite likely represents the most recent mineral growth preserved, which may be attributed to rehydration from crystallization of the last melt.

Summary of deformation and metamorphism

Table 3.3 summarizes the relative chronology of deformation phases and associated metamorphic mineral growth events in Newton Fiord. Figure 3.15 uses a sample from Barrow Peninsula to illustrate the fabrics and key metamorphic minerals associated with each phase of deformation. D_1 is defined by aligned sillimanite inclusions that occur at a high angle to the external S_{2A} foliation. Associated with D_1 was a high-temperature, low-pressure metamorphic event at granulite facies conditions that produced a voluminous garnet-bearing partial melt phase. D_2 was a progressive deformation that began with a regionally-penetrative, bedding-parallel foliation that evolved into kinematically-related regional folding and fold limb shearing. Early D_{2A} gneissic foliation incorporates the partial melt phase (garnet-leucogranite), which is further evidence that extensive partial melting of pelite occurred before the major regional phase of deformation. Associated metamorphic mineral growth is defined by extremely coarse sillimanite and garnet.

The presence of abundant matrix biotite and biotite inclusion trails in late M_2 porphyroblasts indicate that M_2 occurred at upper amphibolite to lower granulite conditions, below the biotite dehydration melting reaction line ("biotite-in"). This necessitates the addition of H_2O to the system, likely from the continued crystallization of melt.

Deformation	Metamorphism	Assemblage	Description
D_1	M_{1A}	Grt + Sil + Crd + Kfs + Il + Qtz +/- Rt	Variably aligned fibrolitic Sil inclusions, at high angle to matrix foliation
	M_{1B}	Crd + Kfs + Pl + Qz + melt +/- Sil +/- Grt	Voluminous partial melt phase, no associated fabric.
D_{2A}	M_{2A}	Grt + Sil + Bt + Kfs + Pl +Il + Qz +/- melt	Main fabric, regionally penetrative, west-dipping, bedding-parallel foliation and associated metamorphic mineral growth.
D_{2B}	M_{2B}	Grt + Sil + Bt + Kfs + Pl +Il + Qz +/- melt	Regional southwest-dipping folds, strong hinge-parallel northwest-plunging lineation, shearing of fold limbs & associated metamorphic mineral growth.

Table 3.3: Summary of relative chronology of deformation phases and associated metamorphic mineral growth events in Newton Fiord.
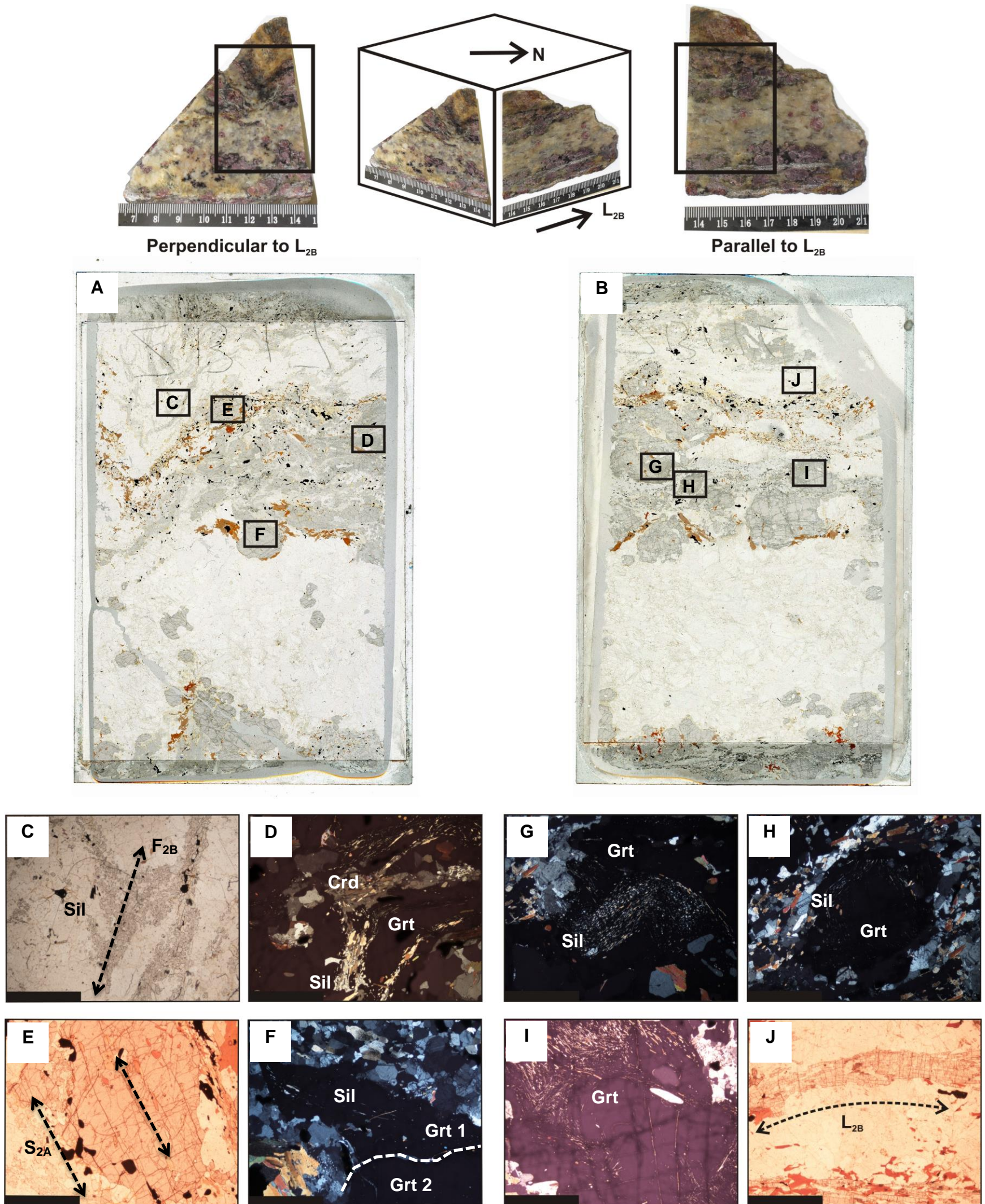
Figure 3.15: Summary diagram of relative chronology of deformation phases and metamorphic events in Newton Fiord. (A) Thin section scan of a sample from Barrow Peninsula that is cut perpendicular to the L_{2B} lineation. (B) Thin section scan the same sample from Barrow Peninsula that is cut parallel to the L_{2B} lineation. Thin sections are 7.5 cm x 5 cm. Boxes indicate location of photomicrographs. (C) Coarse matrix sillimanite is growing in the hinge of an F_{2B} fold, defining the L_{2B} lineation. (D) Medium-grained sillimanite is included in the rims of garnet porphyroblasts and in a cordierite inclusion in the garnet porphyroblast. (E) Garnet porphyroblast that is free of sillimanite inclusions but contains a strong biotite inclusion fabric that is aligned parallel to the external S_{2A} fabric. (F) Two generations of garnet growth. The older garnet ("Grt 1") is irregularly shaped and contains aligned sillimanite inclusions. The younger garnet ("Grt 2") is rounded and free of sillimanite inclusions. The white, dashed line separates the two generations of garnet growth. (G) Garnet porphyroblast containing a crenulated or sigmoidal pattern of fibrolitic sillimanite inclusions, at a high angle to the external S_{2A} foliation. (H) Garnet porphyroblast containing a "starburst" pattern of fibrolitic sillimanite inclusions, at a high angle to the external S_{2A} foliation. (I) Garnet porphyroblast with a "starburst" pattern of fibrolitic inclusion trails, at a high angle to the external S_{2A} foliation. (J) Coarse matrix sillimanite defines the L_{2B} lineation. Scale bar on photomicrographs is 2 mm.

Chapter 4: Preliminary Thermobarometry

INTRODUCTION

Petrography and field relationships revealed textural details necessary to compile a relative chronology of deformation phases and metamorphic mineral growth. Preliminary pressure-temperature (P-T) calculations were undertaken to add quantitative data to the mineral assemblages of each metamorphic event. In order to quantify the pressure and temperature conditions of these metamorphic events, microprobe analyses were done on representative phases of garnet, plagioclase, and biotite. Newton Fiord is not ideal for metamorphic thermobarometry studies because of the extensive partial melting in the region. This work is in addition to the main scope of the thesis and the following data are meant to supplement the petrography.

METHODS

Analyses were done with a JEOL 8200 electron microprobe at Dalhousie University. This instrument has five wavelength-dispersive spectrometers (WDS) and an energy-dispersive spectrometer (EDS). Operating conditions for EDS and WDS spot analyses were 15 kV accelerating voltage and a beam current of 20 nA. Wavelength-dispersive x-ray spectroscopy (WDS) is a quantitative method that uses a diffracting crystal to isolate the characteristic x-ray peaks. This produces a better peak resolution, making interpretation of the data more accurate. The prohibitive aspect to this method is the extensive amount of time required to process a single sample. Energy-dispersive x-ray

spectroscopy (EDS) is a semi-quantitative method that uses a solid-state detector to measure the energy of incoming photons.

Microprobe analyses targeted compositional zoning in garnet porphyroblasts in an attempt to determine the pressure-temperature conditions of M_2. Spot analyses were collected from the core to the rim of garnet porphyroblasts. Biotite and plagioclase inclusions in garnet porphyroblasts and from the matrix were also analysed. WDS point traverses were taken across garnet porphyroblasts that were texturally determined to represent early and late garnet growth stages (Fig. 4.1). Depending on the size of the porphyroblasts, between 10 to 20 points were taken per traverse. Table 4.1 displays representative mineral analyses for garnet, biotite, and plagioclase. In general garnet is relatively to be calcium-poor and iron-rich. Traverse results indicated nearly complete chemical re-equilibration with little variation in elemental concentration from the core to the rim of garnet porphyroblasts. To verify this, several elemental X-ray maps analysing for Na, Ca, K, Mg, Fe, Mn, Si, Al, Zn, and Ti were made of the same porphyroblasts on which
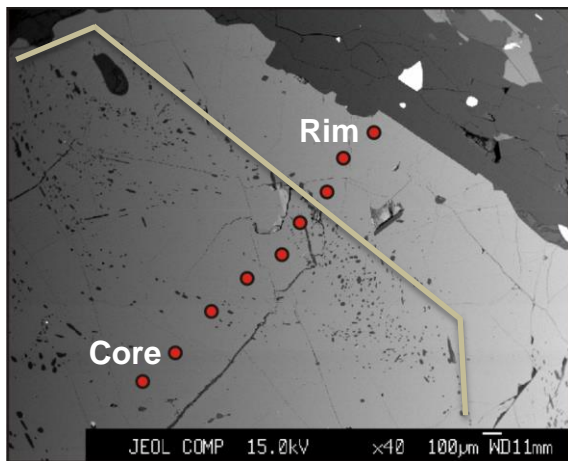

Figure 4.1: Backscatter image of a garnet porphyroblast with red points indicating location of spot analyses from a traverse from core to rim. Garnet porphyroblast was chosen for analysis based on textural evidence of two generations of growth. Tan coloured line indicates edge of early growth rim defined by sillimanite inclusion trails.

the traverses were run (Figs. 4.2 and 4.3). Based on these maps and the point data acquired, a thorough re-equilibration occurred after all identifiable M_1 stages of garnet

growth finished, erasing any compositional zoning. As M_1 is limited to textural evidence, thermobarometry calculations are constrained to M_2 conditions.

Oxides (wt%)	Grt Core Pt. 203	Grt Rim Pt. 92	Bt inclusion Pt. 202	Bt matrix Pt. 122	Pl inclusion Pt. 201	Pl matrix Pt. 121
SiO_2	38.830	39.020	36.830	37.050	60.500	60.360
TiO_2	0.000	0.020	4.820	4.900	0.000	0.000
Al_2O_3	22.410	22.020	16.480	16.290	24.200	24.310
Cr_2O_3	0.060	0.240	0.000	0.050	0.000	0.000
Fe_2O_3	0.000	0.000	0.000	0.000	0.000	0.000
FeO	28.540	30.150	10.480	13.700	0.240	0.000
MnO	0.480	0.400	0.020	0.000	0.000	0.000
MgO	9.270	8.220	16.190	13.820	0.000	0.000
CaO	1.080	1.010	0.000	0.000	5.760	6.180
Na_2O	0.150	0.010	0.190	0.060	8.280	8.080
K_2O	0.050	0.020	8.990	9.840	0.120	0.110
Total	100.870	101.110	94.000	95.710	99.100	99.040
Cations (p.f.u.)						
Si	2.972	2.998	5.442	5.481	2.715	2.709
Ti	0.000	0.001	0.536	0.545	0.000	0.000
Al	2.022	1.994	2.870	2.840	1.280	1.286
Cr	0.004	0.015	0.000	0.006	0.000	0.000
Fe	1.827	1.937	1.295	1.695	0.009	0.000
Mn	0.031	0.026	0.003	0.000	0.000	0.000
Mg	1.058	0.941	3.566	3.048	0.000	0.000
Ca	0.089	0.083	0.000	0.000	0.277	0.297
Na	0.022	0.001	0.054	0.017	0.720	0.703
K	0.005	0.001	1.695	1.857	0.007	0.006
Total	8.029	7.999	15.461	15.488	5.008	5.002

Table 4.1: Representative mineral analyses obtained from electron microprobe and used for P-T estimates. Cations were calculated for the following oxygen atoms per formula unit: garnet = 12, biotite = 22, and plagioclase = 8. Point numbers refer to backscatter images in Figs. 4.4 and 4.5.
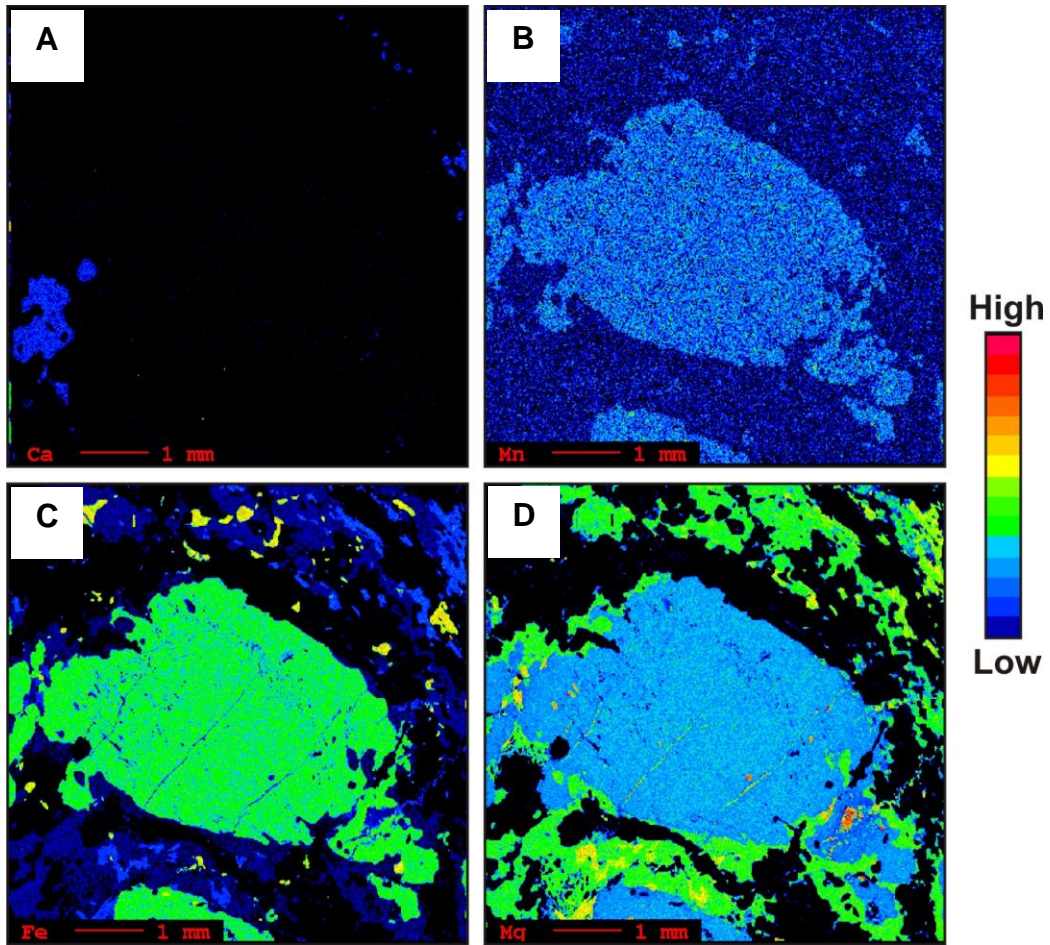
Figure 4.2: Compositional map of the same garnet porphyroblast as Figure 4.1. Maps are of Ca (A), Mn (B), Fe (C), and Mg (D). Complete set of maps including Si, Al, Ti, Na, K, and Zn can be found in Appendix A.
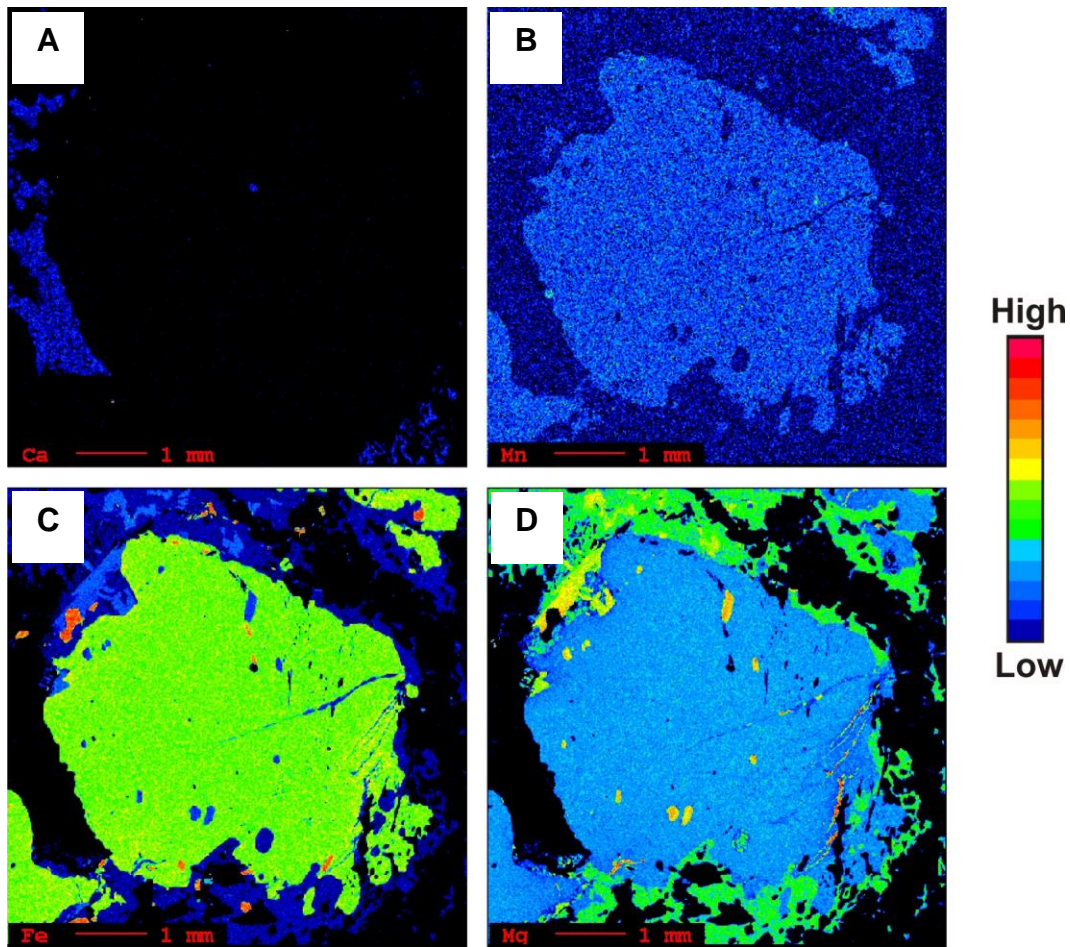
Figure 4.3: Compositional maps of a garnet porphyroblast that texturally preserves an early growth stage. Maps are of Ca (A), Mn (B), Fe (C), and Mg (D). Complete set of maps including Si, Al, Ti, Na, K, and Zn can be found in Appendix A.

THERMOCALC

Average pressure-temperature (P-T) estimates were calculated using the THERMOCALC software (Holland & Powell, 1988) and the internally consistent thermodynamic data set of Holland and Powell (1998). The weight percent of oxides determined from microprobe analysis were first processed using the program AX (Powell & Holland, 1993), which recalculates mineral composition data to generate end-member components. AveragePT mode in THERMOCALC uses these components to determine a series of P-T estimates, which are then averaged to produce a single P-T estimate with a calculated uncertainty (Powell & Holland, 1994).

Due to time constraints the garnet-biotite Fe-Mg cation exchange thermometer (Holdaway, 2000) and the garnet-aluminosilicate-plagioclase barometer (GASP; Holdaway, 2001) were used in THERMOCALC for simplicity. Retrograde Fe-Mg exchange between garnet and biotite grains that are in direct contact is responsible for a significant amount of error, which generally results in minimum temperatures estimates, as opposed to maximums. After Holdaway (2001), results obtained using samples with low grossular (<3% Grs) and low anorthite (<17% An) content should be treated with caution. As these rocks are interpreted to be initially calcium-poor and iron- and titanium-rich, there are considerable errors to take into consideration with respect to the chosen thermometer and barometer.

RESULTS – M$_{2A}$

Based on petrography M$_{2A}$ has an assemblage of garnet + sillimanite + biotite + ilmenite + K-feldspar + plagioclase + quartz +/- melt. Figure 4.4 shows a scan of the thin section

from which these analyses were done. The backscatter image illustrates where point analyses were collected to obtain the data for average P-T calculations. This sample was chosen because it contains garnet porphyroblasts that are free of sillimanite inclusions and have aligned inclusions of biotite. Using compositional data from the core of the garnet porphyroblast and inclusions of biotite and plagioclase in the core of the same garnet porphyroblast, a temperature of 650°C ± 109°C and a pressure of 5.3 Kbar ± 1.8 Kbar were calculated. These values are weighted mean averages ± the standard deviation between results generated from each equation used by THERMOCALC. Due to Fe-Mg exchange between the biotite and the garnet, which are in direct contact, this temperature is considered a minimum estimate.
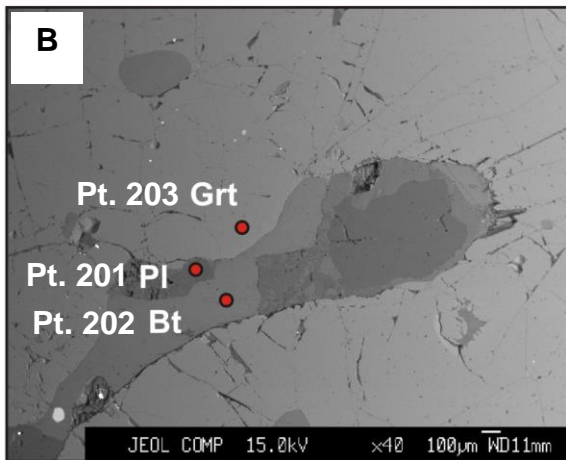
Figure 4.4: (A) Thin section scan of a sample from Sillimanite Ridge. Black box indicates location of backscatter image. (B) Backscatter image of garnet porphyroblast with an inclusion of plagioclase and biotite. Red points indicate location of spot analyses used for average P-T calculations. Analysis point numbers refer to Table 4.1.

RESULTS – M$_{2B}$

Based on petrography M$_{2B}$ has an assemblage of garnet + sillimanite + biotite + ilmenite + K-feldspar + plagioclase + quartz +/- melt. Figure 4.5 shows a scan of the thin section from which these analyses were done. The backscatter image illustrates where point

analyses were collected to obtain the data for average P-T calculations. This sample was chosen because texturally, it clearly represents a group of M_2 garnets. It was cut parallel to L_{2B} and garnet porphyroblasts are oblate. Using compositional data from the rim of a garnet porphyroblast, matrix biotite and matrix plagioclase, a temperature of 750°C ± 130°C and a pressure of 5.9 Kbar ± 2 Kbar were calculated. These values are weighted mean averages ± the standard deviation between results generated from each equation used by THERMOCALC.
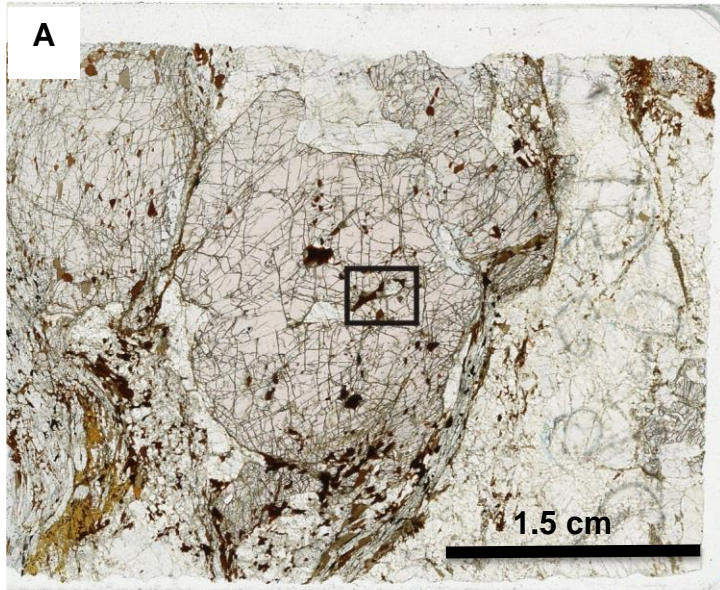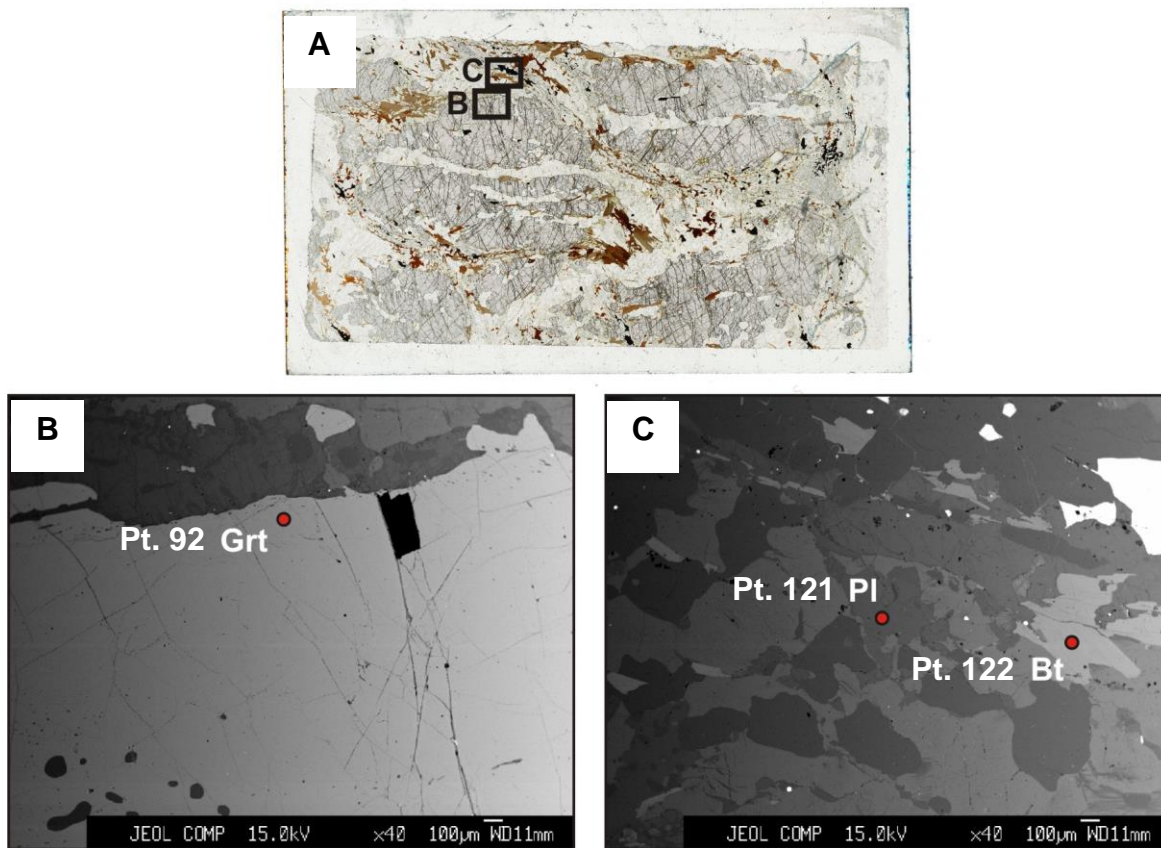

Figure 4.5: (A) Thin section scan of a sample from Barrow Peninsula. Black boxes indicate location of backscatter images. (B) Backscatter image of rim of garnet porphyroblast. (C) Backscatter image of plagioclase and biotite in the matrix near the garnet porphyroblast shown in (B). Red points indicate locations of spot analyses used for average P-T calculations. Thin section is 4.5 cm x 2.5 cm. Analysis point numbers refer to Table 4.1.

UNCERTAINTY

These data are a preliminary attempt to quantify the relative P-T conditions indicated by petrography. Further calculations, on a wider and more representative distribution of samples, are necessary to verify these results.

Another potential source of error for M_{2B} is the generation of plagioclase in matrix, as it is indistinguishable from M_{1B} plagioclase. There are very few plagioclase grains in the matrix that can be considered to be in textural equilibrium with surrounding mineral phases. Plagioclase is not particularly susceptible to retrograde chemical exchange and may therefore preserve different compositions. Further work is required to determine with which mineral phases plagioclase is in equilibrium.

Also, the effects of elevated iron and titanium on P-T estimates and on the Fe-Mg exchange thermometer have not been fully studied and could add significantly to the error of these calculations.

With more time, other mineral thermometers and barometers would be considered. For instance, the proportions of sodium and potassium in cordierite have been shown to be a reasonable thermometer in anatectic pelites (Thomson et al., 2002).

Chapter 5: Discussion

The relative chronology of deformation and metamorphism in Newton Fiord has been established and further enhanced by preliminary P-T calculations for M_2. These data will now be used to construct a pressure-temperature-deformation (P-T-d) path for Newton Fiord. Future work that considers Hall Peninsula must honour these textural data and consider the following interpreted P-T-d path.

P-T-D PATH FOR NEWTON FIORD

Mineral compositions and P-T conditions are fundamentally linked, and when placed in the context of a petrogenetic grid, a path chronicling the sequence of metamorphism and deformation can be determined. The NaKFMASH petrogenetic grid was used after Spear (1999) who used it to model the P-T paths of anatectic pelites (Fig. 5.1). This system includes the components Na_2O-K_2O-FeO-MgO-Al_2O_3-$SiO2$-H_2O. The addition of a calcium component does not introduce any new phases into the system and for that reason it has been omitted (Spear, 1999).
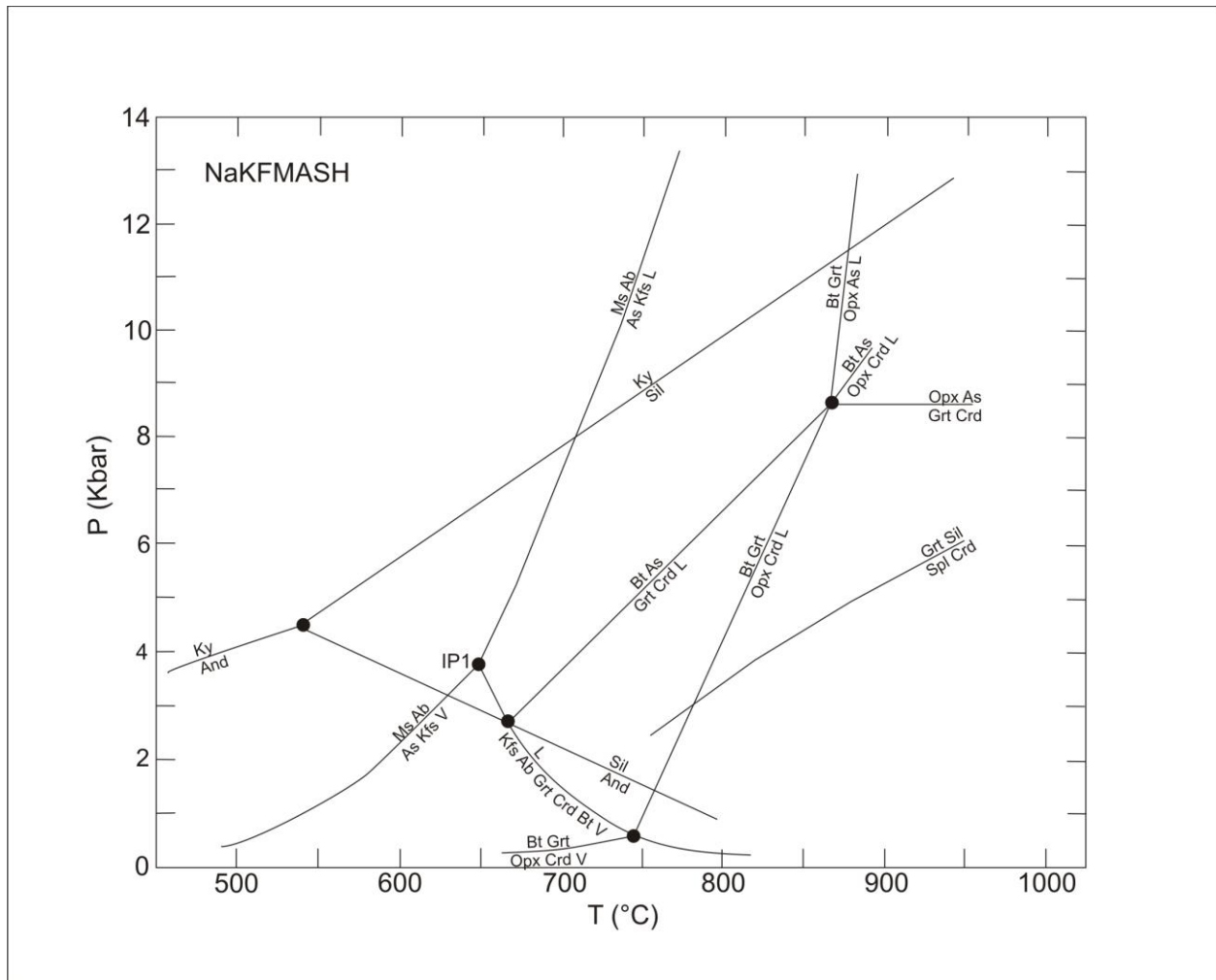
Figure 5.1: Petrogenetic grid with the phases present based on components of Na$_2$O-K$_2$O-FeO-MgO-Al$_2$O$_3$-SiO2-H$_2$O. "IP1" stands for invariant point 1. See text for description of P-T grid. After Spear, 1999.

Spear (1999) outlines three assumptions, with respect to the function of the H$_2$O vapour phase in the system, that are essential to interpreting the P-T path of anatectic pelites using the NaKFMASH petrogenetic grid. First it is assumed that no water is added externally and all water present in the system is derived from the dehydration of hydrous minerals. Second, it is assumed that all water produced from dehydration leaves the rock, in other words there is a vapour phase present, but in "vanishingly small quantities". Third, it is assumed that once the rock has begun to melt, no water is lost

from the system but that all water from dehydration is dissolved in the melt. Based on these assumptions dehydration melting is favoured and vapour-saturated melting is not stable, with the exception of the minimum-melting reaction of the system (Spear, 1999).

By combining field data, petrography and mineral chemistry, a model for the evolution of Newton Fiord has been developed. This model will be described in terms of a relative pressure-temperature-deformation path in the context of the NaKFMASH petrogenetic grid for anatetic pelites after Spear (1999).

1. D_1/M_1: HIGH TEMPERATURE/LOW PRESSURE

Calculations for M_1 metamorphic conditions are limited by the thorough chemical re-equilibration after the partial melt phase and long-lasting D_{2A} deformation and M_{2A} metamorphism. Despite these limitations, a region of relative pressure-temperature conditions can be determined based on the preserved mineral assemblages of M_{1A}: garnet + sillimanite + K-feldspar + ilmenite + quartz +/- rutile (+/- spinel?) and of M_{1B}: plagioclase + cordierite + K-feldspar + quartz + garnet +/- sillimanite. These assemblages are interpreted to have originally equilibrated beyond the biotite dehydration melting reaction line. In Figure 5.2 the P-T conditions and interpreted path attributed to D_1/M_1 is shown. The purple circle represents the region of P-T space interpreted to reflect the mineral assemblages of M_{1A} and M_{1B}. Melt textures, the presence of abundant cordierite, sillimanite inclusions and rare spinel indicate high temperature high temperature and low pressure metamorphism. The lack of biotite in garnet porphyroblasts that contain sillimanite inclusion trails at a high angle to the external fabric, also suggest high temperature equilibration ("biotite-out").
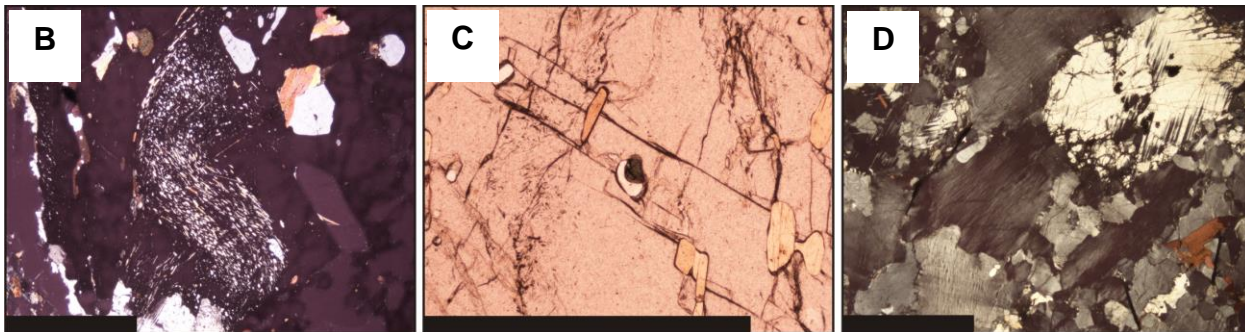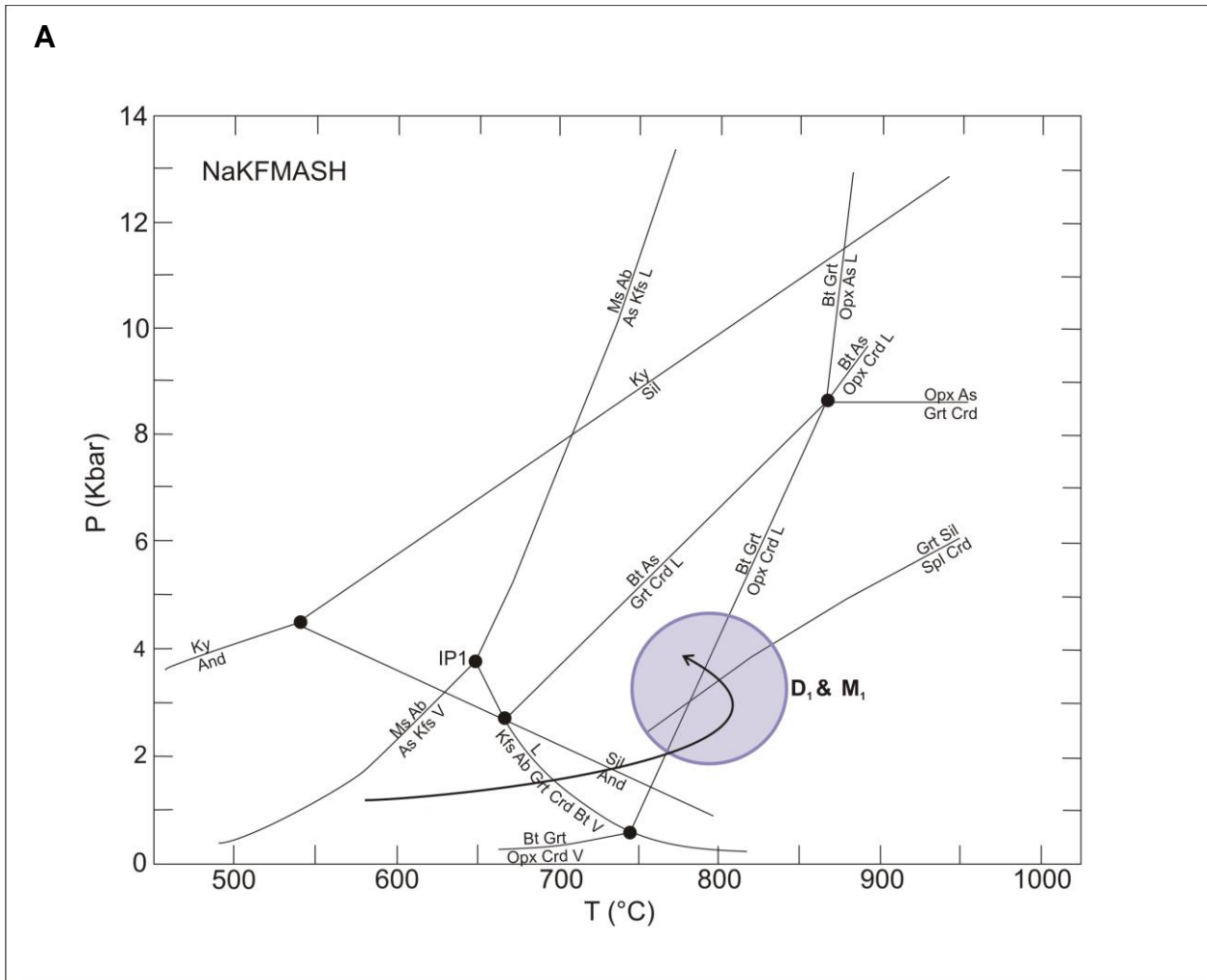
Figure 5.2: (A) Relative P-T path of early high-temperature, low-pressure deformation and associated metamorphism. NaKFMASH grid, after Spear, 1999. (B) Photomicrograph of early sillimanite inclusion trails. (C) Photomicrograph of green spinel inclusion in garnet. (D) Photomicrograph of cordierite, a relatively high-temperature mineral. Scale bar is 2 mm.

These high temperature-low pressure assemblages are consistent with contact metamorphism as a consequence of plutonic intrusion at shallow structural levels. The emplacement temperature of magmatic orthopyroxene-bearing monzogranite has been

determined to be about 750-850°C (Kilpatrick & Ellis, 1992), which is consistent with the temperatures suggested by preserved M_1 assemblages. Contact metamorphism traditionally obliterates pre-existing tectonic fabrics, and yet there is clearly a preserved foliation associated with M_1.

The early foliation, S_1, likely reflects early onset of orogenesis just prior to and during emplacement of the charnockite. Alternatively, the early fabric may represent strain imposed by emplacement of the charnockite. Further work is required in order to determine if D_1 is related to collisional processes or if it is a result of pluton emplacement.

2. D_{2A}/M_{2A}: REGIONAL DEFORMATION AND METAMORPHISM

D_{2A} is associated with the strong bedding-parallel fabric, which is the main foliation that defines the map pattern of Hall Peninsula. M_{2A} has a mineral assemblage of garnet + sillimanite + biotite + ilmenite + K-feldspar + plagioclase + quartz +/- melt and equilibrated at biotite-in upper amphibolite to lower granulite facies conditions. Preliminary P-T estimates for M_{2A} give an approximate temperature of 650°C ± 109°C and an approximate pressure of 5.3 Kbar ± 1.8 Kbar. The error on these calculations is significant and it may not be reasonable to accept these data as accurate, however the P-T path suggested by the addition of this point on the grid represents a plausible sequence of events. D_{2A} and M_{2A} represent the beginning of a more typical orogenic clockwise prograde P-T path. The relative P-T path indicates that these rocks could have passed back into the muscovite stability field, however the distinct absence of any

muscovite, particularly any muscovite inclusions in porphyroblasts, suggests that D_{2A}/M_{2A} did not pass below the muscovite-in line.

Figure 5.3 shows the interpreted P-T conditions attributed to D_{2A}/M_{2A} and path from earlier high temperature contact metamorphism. The purple circle represents the region of P-T space suggested by the mineral assemblage of M_{2A}, which coincides well with the P-T estimates. D_{2A}/M_{2A} can be reasonably attributed to early crustal stacking during orogenesis. This deformation affects both the charnockite and the garnet-leucogranite partial melt phase.

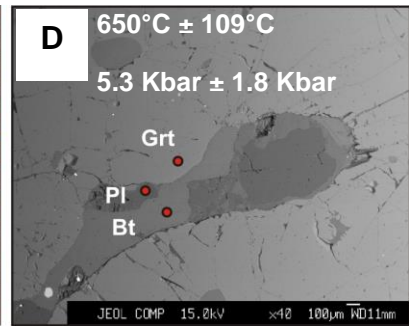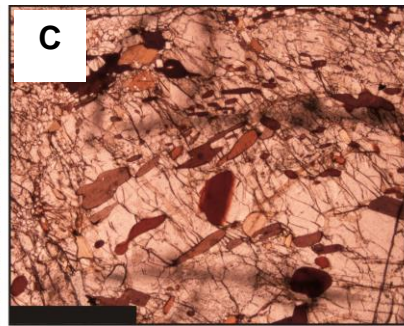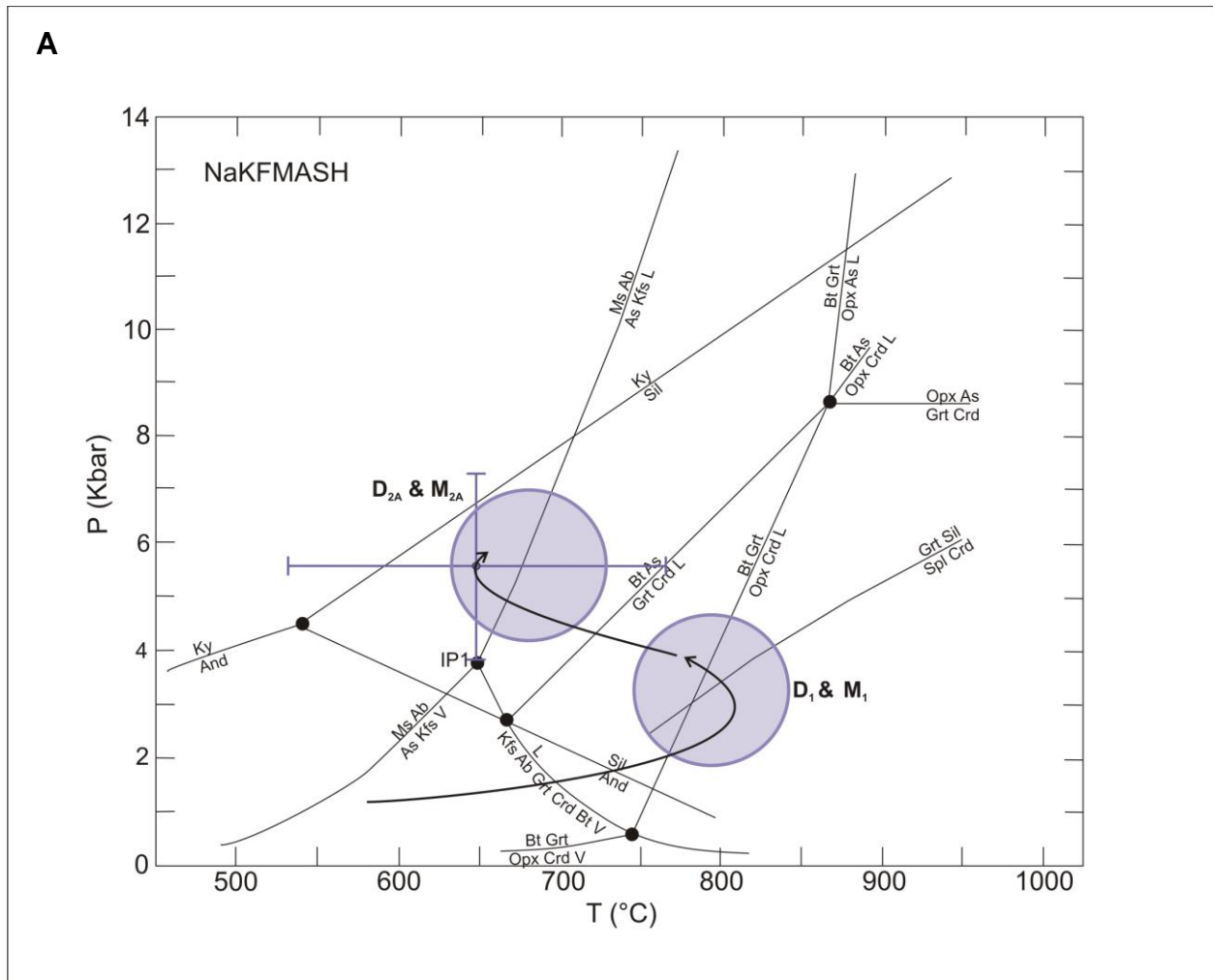Figure 5.3: (A) Relative P-T path of D_{2A}/M_{2A} deformation and associated metamorphism. NaKFMASH grid, after Spear, 1999. (B) Field photo of regional foliation. Hammer is 40 cm in length, wooden handle points north. (C) Photomicrograph of biotite inclusion trails. (D) Backscatter image of garnet, plagioclase and biotite analysed for average P-T calculations. Scale bar on photomicrograph is 2 mm.

D_{2A} marks the transition from early deformation synchronous with charnockite emplacement to crustal stacking related to collisional processes. The specific crustal blocks involved and the plate motions are still unclear but are part of an ongoing mapping and research effort related to the CNGO Hall Peninsula project.

3. D_{2B}/M_{2B}: BASEMENT-INVOLVED FOLDING

Regional folding and shearing of fold limbs characterize the later phase of progressive D_2 deformation. D_{2B} is expressed as a strong hinge-parallel lineation defined by coarse matrix sillimanite and biotite. M_{2B} has the same preserved mineral assemblage as M_{2A}, garnet + sillimanite + biotite + ilmenite + K-feldspar + plagioclase + quartz +/- melt. Preliminary P-T estimates for M_{2B} suggest an approximate temperature of 750°C ± 130°C and an approximate pressure of 6 Kbar ± 2 Kbar. Figure 5.4 shows the P-T conditions attributed to D_{2B}/M_{2B} and the interpreted path from D_1. The purple circle represents the region of P-T space suggested by the mineral assemblage of M_{2B} and the error bars indicate the P-T calculations for M_{2B}.

D_2 was a progressive deformation that began with D_{2A}, which resulted in west-dipping foliation likely as a result of extensive tectonic stacking. This was followed by D_{2B}, which resulted in west-dipping basement-involved folding with strong hinge-parallel extension and fold-limb shearing. D_{2B} likely represents progression into thick-skinned deformation during continued east-verging compression.

The D_{2B} variation in strain is reflected in the regional map pattern of the western domain of Hall Peninsula. Regional folds vary from large and open and to tight or isoclinal with

local shearing. Newton Fiord displays on a smaller scale a pattern that is common to a large portion of Hall Peninsula.

The actual volume proportion of melt at each study site is difficult to estimate due to the intensity of post-leucosome strain. At first glance there appears to be more melt present at Barrow Peninsula but in reality there is a significant amount of melt present at Sillimanite Ridge as well, it is just better interlayered with the pelite and psammite due to D_{2B} transposition.

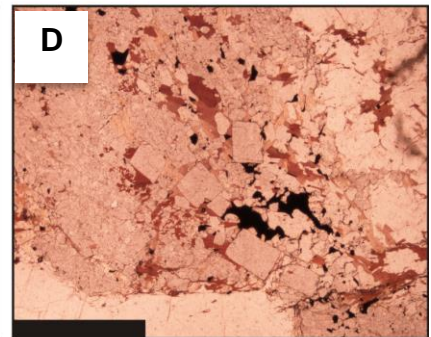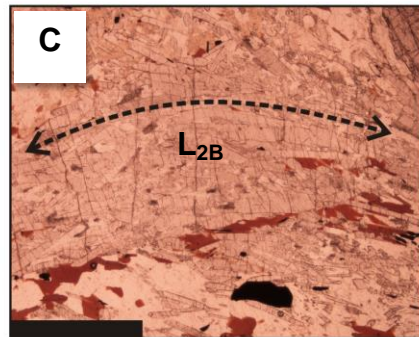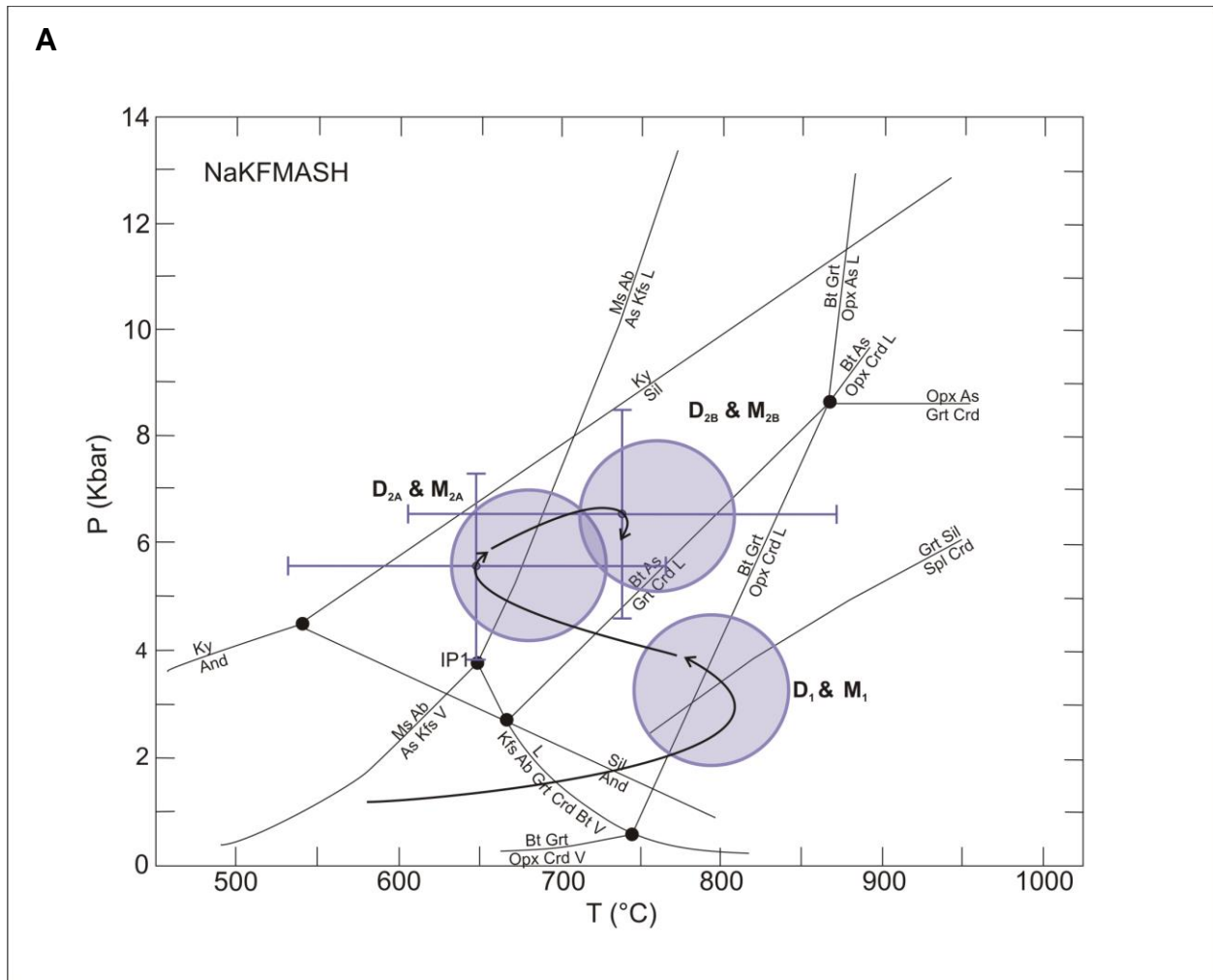Figure 5.4: (A) Relative P-T path of D_{2B}/M_{2B} deformation and associated metamorphism. NaKFMASH grid, after Spear, 1999. (B) Thin section scan of pelite showing an F_{2B} fold. (C) Photomicrograph of coarse matrix sillimanite defining the L_{2B} regional lineation. (D) Photomicrograph of coarse matrix sillimanite, cut perpendicular to the L_{2B} regional lineation. Scale bar is 2 mm.

4. RETROGRADE PATH

In Newton Fiord and the western domain of Hall Peninsula, there is a striking lack of muscovite. According to the P-T grid of Spear (1999) the lack of muscovite suggests that the rocks cooled below Invariant Point 1 (IP1; Fig. 5.5). If they had cooled above IP1, retrograde muscovite would have been produced at the expense of K-feldspar (Spear, 1999). Below IP1 melt crystallization will occur, releasing free water, which presumably leaves the rock. This eliminates the water necessary for retrograde muscovite to form and K-feldspar will be preferentially preserved (Spear, 1999). As shown in Figure 5.5 the predicted cooling path for Newton Fiord is below IP1 in order to preserve K-feldspar and explain the lack of muscovite.
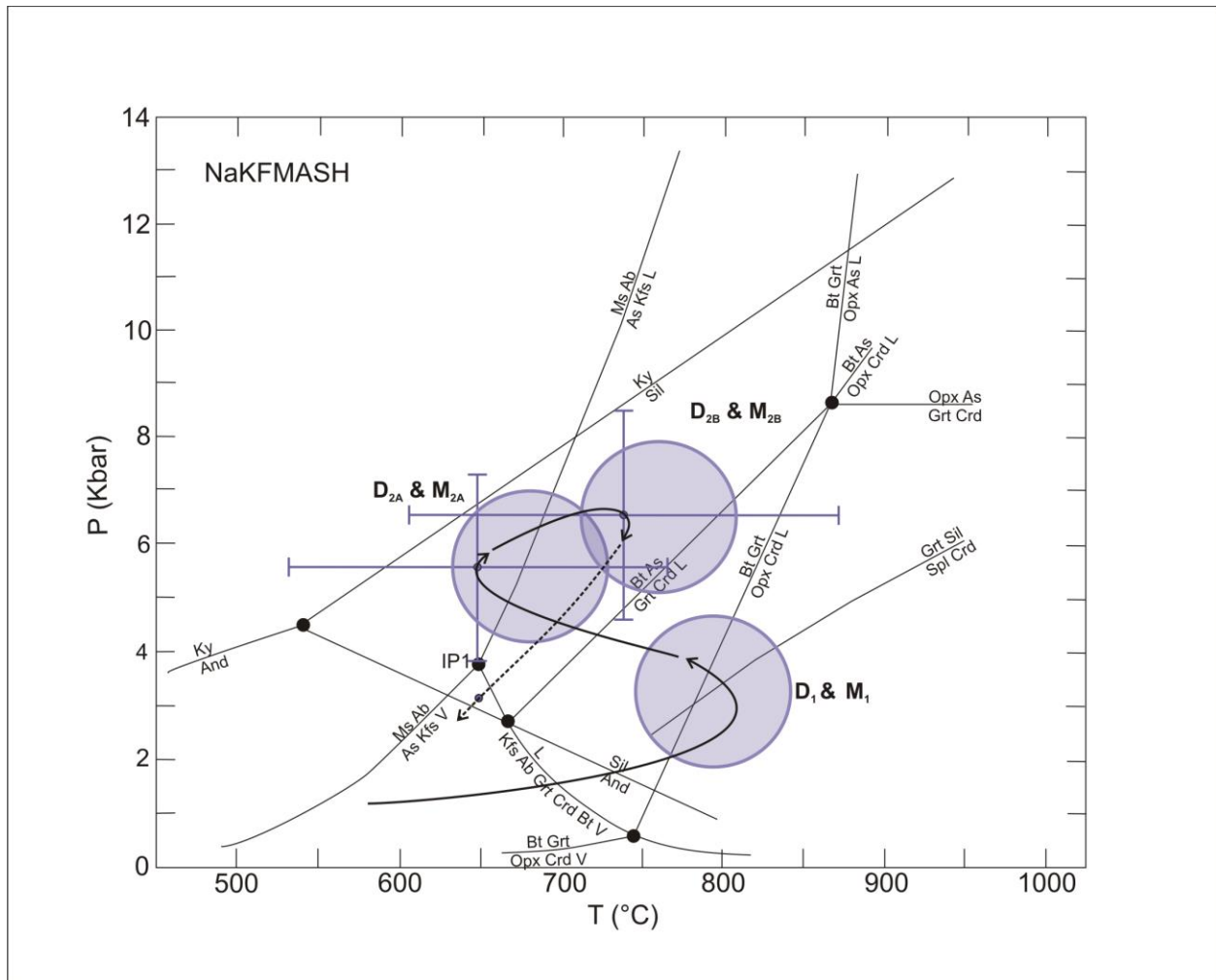
Figure 5.5: Relative retrograde P-T path. NaKFMASH grid, after Spear, 1999.

ALTERNATIVE P-T-D PATH & OTHER CONSIDERATIONS

The calculations for M_{2A} represent at best a minimum because the composition of biotite has likely been reset due to retrograde Fe-Mg exchange. The standard deviations of M_{2A} and M_{2B} overlap considerably and may be quantitatively indistinguishable. In terms of a strict P-T path this data could also be represented as a single continuous counter-clockwise path (Fig. 5.6). It is the textural observations that add weight to an early

counter-clockwise path followed by a later clockwise path, joined because deformation is continuous throughout the different metamorphic events.

Figure 5.6: Alternative continuous counter-clockwise path. NaKFMASH grid after Spear 1999.

The petrogenetic grid by Spear (1999) is based on an Fe/Mg ratio of 0.8. The data used for P-T calculations in this thesis produced an Fe/Mg ratio of closer to 0.6. This lower Fe/Mg ratio is further evidence that M_{2A} calculations represent at best a minimum temperature estimate.
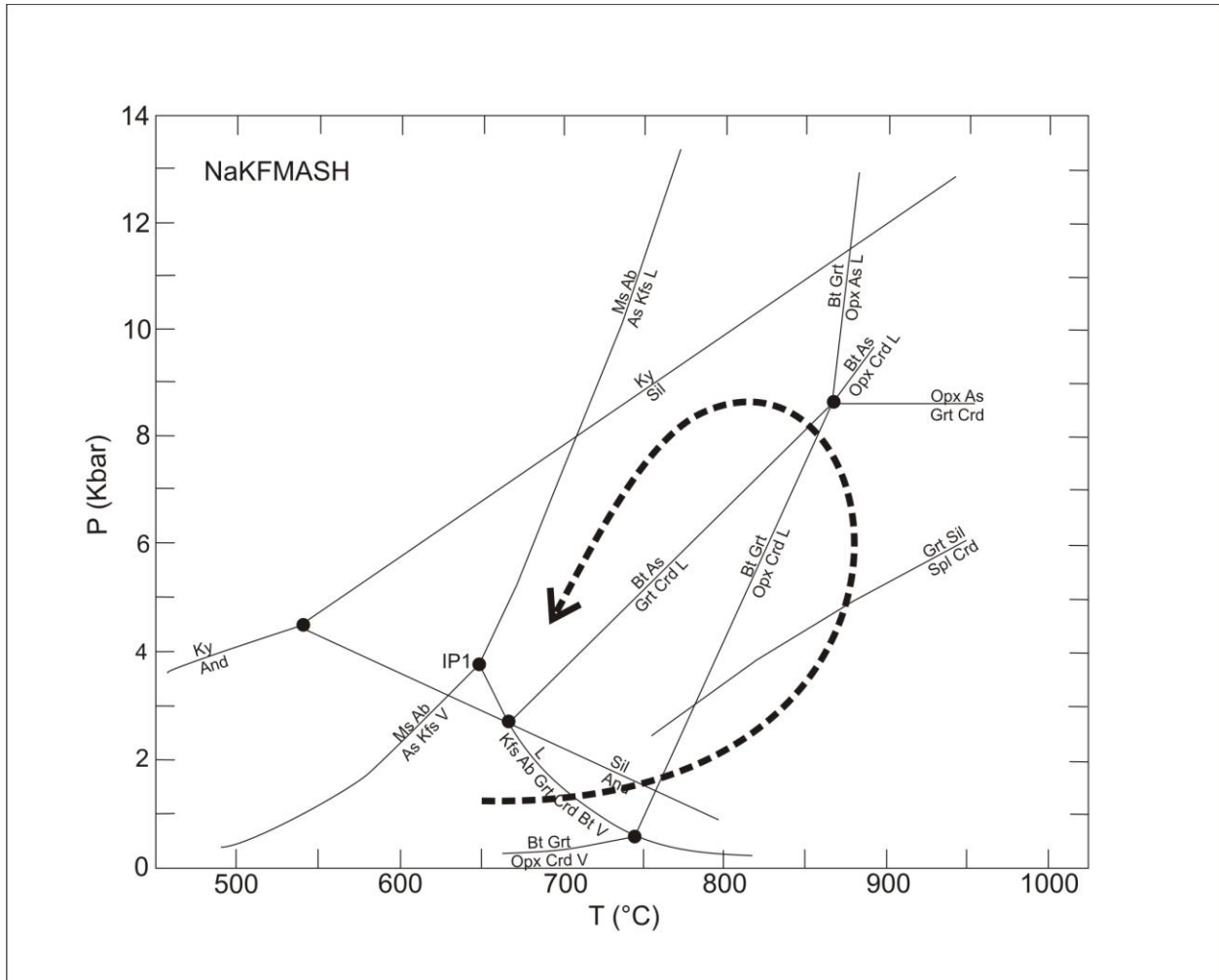
REGIONAL IMPLICATIONS

This study does not intend to suggest that all of Hall Peninsula conforms to such an unusual P-T path as presented by the above data. It is predicted that the eastern lithological domain of Hall Peninsula retains a clockwise prograde P-T path that is typical of large collisional orogens. The charnockite is restricted to the western domain (refer to Fig. 1.2) and to date cordierite-bearing rocks have not been observed in the eastern domain of Hall Peninsula. It is reasonable to assume that the eastern domain was outside of the thermal aureole attributed to charnockite emplacement and did not experience the same early high-temperature contact metamorphism as the western domain. It is unclear whether the early deformation in Newton Fiord (D_1) also affected rocks in the eastern domain. If so, D_1 would more likely represent early orogenesis rather than strain imposed by pluton emplacement.

The observations made in Newton Fiord can be used to help interpret the regional map pattern of seemingly random distribution of tight to open folds across the western domain of Hall Peninsula. The progressive deformation from regionally-penetrative foliation to regional basement-involved folding is similarly expressed on both Cumberland Peninsula and in South Baffin. On Cumberland this deformation has been dated between 1860-1840 Ma and in South Baffin it has been dated between 1850-1835 Ma. The specific timing of D_2 deformation remains unknown on Hall Peninsula; it is the focus of ongoing geochronological studies. Both Cumberland Peninsula and South Baffin have dominantly south-verging structures, which begs the question: why are structures on Hall Peninsula east-verging? It is also of note that the early fabric

associated with D_1 deformation is present on Cumberland Peninsula, but there is no corresponding fabric in South Baffin.

CONCLUSIONS

Petrography and field relationships revealed three fabrics and four separate phases of mineral growth. D_1/M_{1A} represents early fabric formation and contact metamorphism at high temperature, low pressure likely related to charnockite emplacement. S_1 could be a result of early onset of orogensis or strain imposed by charnockite emplacement. M_{1B} represents a voluminous partial melt phase attributed to the heat outlasting deformation as a result of M_{1A} contact metamorphism. D_2 is a progressive deformation beginning with a bedding-parallel, regionally penetrative foliation that evolved into regional folding and related limb shearing. M_2 is the metamorphic mineral growth associated with progressive D_2 deformation. D_2/M_2 represents a major phase of deformation that was likely a result of crustal stacking during continental collision of yet-to-be-determined crustal blocks.

RECOMMENDATIONS

1. Pseudosections: The P-T estimates undertaken in this study were simply a supplementary endeavour and not the main focus of this thesis. Time restrictions placed heavy constraints on the amount of data processed with THERMOCALC. To improve the quantitative resolution of the Newton Fiord P-T path, more detailed thermobarometry is recommended. Provided the melt phase can be accounted for, pseudosections would likely provide the most accurate P-T model.

2. Geochronology: Beyond adding more quantitative pressure and temperature data, the addition of concrete ages would add insight to the timing of deformation and metamorphism at Newton Fiord and allow for regional calibration of events. The Newton Fiord migmatites are ideal candidates for LA-ICPMS dating of in-situ monazite phases, as there are multiple stages of monazite growth preserved throughout the samples.

References

Bell, T. H., Johnson, S. E., Davis, B., Forde, A., Hayward, N. and Wilkins, C. (1992). Porphyroblast inclusion-trail orientation data: eppure non son girate. Journal of Metamorphic Geology, 10: p. 295-307.

Berman, R. G., Sanborn-Barrie, M., Hamilton, B. M., Rayner, N. and Young, M. (2013). Preliminary in situ SHRIMP geochronological constraints on the tectonometamorphic evolution of Cumberland Peninsula, Baffin Island.

Blackadar, R.G. (1967). Geological Reconnaissance, southern Baffin Island, District of Franklin. Geological Survey of Canada Paper 66-47.

Corrigan, D., Pehrsson, S., Wodicka, N. and de Kemp, E. (2009). The Paleoproterozoic Trans-Hudson Orogen: a prototype of modern accretionary processes. Geological Society, London, Special Publications, 327: p.457-479.

Dumont, R. and Dostaler, F. 2010b. Geophysical Series, NTS 25-I/NE, Aeromagnetic Survey Hall Peninsula, Nunavut; Geological Survey of Canada, Open File 6414, scale 1:100 000.

Dumont, R., and Dostaler, F. 2010c. Geophysical Series, NTS 25-I/NW, Aeromagnetic Survey Hall Peninsula, Nunavut; Geological Survey of Canada, Open File 6415, scale 1:100 000.

Dumont, R., and Dostaler, F. 2010d. Geophysical Series, NTS 25-J/NE, Aeromagnetic Survey Hall Peninsula, Nunavut; Geological Survey of Canada, Open File 6416, scale 1:100 000.

Dumont, R., and Dostaler, F. 2010e. Geophysical Series, NTS 25-O/SE, Aeromagnetic Survey Hall Peninsula, Nunavut; Geological Survey of Canada, Open File 6417, scale 1:100 000.

Dumont, R., and Dostaler, F. 2010f. Geophysical Series, NTS 25-O/SW, Aeromagnetic Survey Hall Peninsula, Nunavut; Geological Survey of Canada, Open File 6418, scale 1: 100 000.

Dumont, R., and Dostaler, F. 2010g. Geophysical Series, NTS 25-O/NE, Aeromagnetic Survey Hall Peninsula, Nunavut; Geological Survey of Canada, Open File 6419, scale 1: 100 000.

Dumont, R., and Dostaler, F. 2010h. Geophysical Series, NTS 25-O/NW, Aeromagnetic Survey Hall Peninsula, Nunavut; Geological Survey of Canada, Open File 6420, scale 1: 100 000.

Dumont, R., and Dostaler, F. 2010i. Geophysical Series, NTS 25-P/SE, Aeromagnetic Survey Hall Peninsula, Nunavut; Geological Survey of Canada, Open File 6421, scale 1: 100 000.

Dumont, R., and Dostaler, F. 2010j. Geophysical Series, NTS 25-P/SW, Aeromagnetic Survey Hall Peninsula, Nunavut; Geological Survey of Canada, Open File 6422, scale 1: 100 000.

Dumont, R., and Dostaler, F. 2010k. Geophysical Series, NTS 25-P/NE, Aeromagnetic Survey Hall Peninsula, Nunavut; Geological Survey of Canada, Open File 6423, scale 1: 100 000.

Dumont, R., and Dostaler, F. 2010l. Geophysical Series, NTS 25-P/NW, Aeromagnetic Survey Hall Peninsula, Nunavut; Geological Survey of Canada, Open File 6424, scale 1: 100 000.

Fossen, H. (2010). Structural Geology. Cambridge University Press, United Kingdom. Ch. 12, Ch. 13.

Hoffman, P.F. (1988). United Plates of America, the birth of a craton: early Paleoproterozoic assembly and growth of Laurentia. Annual Review of Earth Planetary Sciences, 16: p.543-603.

Holdaway, M. J. (2000). Application of new experimental and garnet Margules data to the garnet–biotite geothermometer. American Mineralogist 85: p.881–892.

Holdaway, M. J. (2001). Recalibration of the GASP geobarometer in light of recent garnet and plagioclase activity models and versions of the garnet–biotite geothermometer. American Mineralogist 86: p.1117–1129.

Holland, TJB, & Powell, R. (1998). An internally-consistent thermodynamic dataset for phases of petrological interest. Journal of Metamorphic Geology 16: p.309–344.

Kilpatrick, J. A. & Ellis, D. J. (1992). C-type magmas: igneous charnockites and their extrusive equivalents.Transactions of the Royal Society of Edinburgh, 83: p.155-164.

Kretz, R. (1983). Symbols for rock-forming minerals. American Mineralogist, 68: p.277-279.

Machado, G., Bilodeau, C., Takpanie, R., St-Onge, M.R., Rayner, N.M., Skipton, D.R., From, R.E., MacKay, C.B., Creason C.G. and Braden, Z.M. (2013). Hall Peninsula regional bedrock mapping, Baffin Island, Nunavut: summary of fieldwork; in Summary of Activities 2012, Canada-Nunavut Geoscience Office, p. 13–22.

Passchier, C. W., Trouw, R. A. J., Zwart, H. J. & Vissers, R. L. M. (1992). Porphyroblast rotation: eppur si muove? Journal of Metamorphic Geology, 10: p. 283-294.

Passchier, C. W. & Trouw, R. A. J. (2005). Microtectonics, 2nd edition. Springer-Verlag Berlin Heidelberg, Germany. Ch. 3, 4 & 7.

Powell, R & Holland, T.J.B. (1993). On the formulation of simple mixing models for complex phases. American Mineralogist 78: p.1174–1180.

Powell, R, & Holland, TJB, (1994). Optimal geothermometry and geobarometry. American Mineralogist, 79: p.120-133.

Powell, R, & Holland, TJB. (1988). An internally consistent thermodynamic dataset with uncertainties and correlations: 3: application methods, worked examples and a computer program. Journal of Metamorphic Geology, 6: p.173–204.

Powell, R. & Holland, T.J.B. (2008). On thermobarometry. Journal of Metamorphic Geology, 26: p.155–179.

Ramsay, J. G. & Huber, M. I. (1983). The techniques of modern structural geology, Volume 1: Strain Analysis. Academic Press, London, United Kingdom.

Sanborn-Barrie, M., St-Onge, M. R., Young, M.D. & James, D.T. (2008). Bedrock geology of southwestern Baffin Island, Nunavut: expanding the tectonostratigraphic framework with relevance to mineral resources. Geological Survey of Canada Current Research, 2008-6, 1-16.

Sawyer, E. W. (2008). Working with migmatites: Nomenclature for the constituent parts. Working with Migmatites, Mineralogical Association of Canada Short Course Series, 38: p.1-28.

Scott, D.J. (1996) Geology of the Hall Peninsula east of Iqaluit, southern Baffin Island. Current Research 1996-C, Geological Survey of Canada, 1996-C, 83-91.

Scott, D.J. (1999) U-Pb geochronology of the eastern Hall Peninsula, southern Baffin Island, Canada: a northern link between the Archean of West Greenland and the Paleoproterozoic Torngat Orogen of northern Labrador. Precambrian Research, 93: p.5-26.

Spear, F. S., Kohn, M. J. & Cheney, J. T. (1999). P-T paths from anatectic pelites. Contributions to Mineral Petrology 134: p.17-32.

St-Onge, M., Scott, D.J. & Lucas, S.B. (April 2000). Early partitioning of Quebec: Microcontinent formation in the Paleoproterozoic. Geology, 28: p.323-326.

St-Onge, M., Scott, D.J. & Wodicka, N. (2001). Terrane boundaries within the Trans-Hudson Orogen (Quebec-Baffin segment), Canada: changing structural and metamorphic character from foreland to hinterland. Precambrian Research, 107: p.75-91.

St-Onge, M.R., Van Gool, J.A.M., Garde, A.A. & Scott, D.J. (2009) Correlation of Archean and Paleoproterozoic units between northeastern Canada and estern Greenland: constraining the pre-collisional upper plate accretionary history of the Trans-Hudson orogen. Geological Society, London, Special Publication, 318: p.193-235. doi:10.1144/SP318.7

St-Onge, M. R., Hanmer, S. & Scott, D. J.(1996). Geology of the Meta Incognita Peninsula, south Baffin Island, Northwest Territories; tectonostratigraphic units and regional correlations. Current Research – Geological Survey of Canada, p.63-72.

Thompson, P., Harley, S. L. & Carrington, D. P. (2002). Sodium and potassium in cordierite a potential thermometer for melts?. European Journal of Mineralogy, 14: p. 459-469.

Tremblay, T., Leblanc-Dumas, J., Allard, M., Gosse, J.C., Creason, C.G., Peyton, P., Budkewitsch, P. & LeBlanc, A-M. 2013: Surficial geology of southern Hall Peninsula, Baffin Island, Nunavut: summary of the 2012 field season; in Summary of Activities 2012, Canada Nunavut Geoscience Office, p. 93–100.

van Gool, J. A. M., Connelly, J. M., Marker, M. & Mengel, F. C. (2002). The Nagssugtoqidian Orogen of West Greenland: tectonic evolution and regional correlations from a West Greenland perspective. Canadian Journal of Earth Sciences, 39: p.665-686.

Wardle, R. J., James, D. T., Scott, D. J. & Hall, J. (2002). The southeastern Churchill Province: Synthesis of a Paleoproterozoic transpressinal orogeny. Canadian Journal of Earth Sciences, 39: p. 639-663.

Whalen, J.B., Wodicka, N., Taylor, B.E., Jackson, G.D. (2010). Cumberland batholith, Trans-Hudson Orogen, Canada: Petrogenesis and implications for Paleoproterozoic crustal and orogenic processes. Lithos, 117: p.99-118.

Winter, J. D. (2010). Principles of igneous and metamorphic petrology, 2nd edition. Pearson Prentice Hall, United States of America, Ch. 23.

Yardley, B. W. D. (1989). An introduction to metamorphic petrology. Longman Singapore Publishers, United Kingdom, Ch. 3.

Appendix A: Compositional maps